Combining measured on-board Sport Utility Vehicle (SUV) emissions in real driving conditions with geo-computation methods to create real-world vehicle emission factors

R. Smit [a,b,c*], M. Awadallah[b], S. Bagheri[b], N. C. Surawski[b]

[a] Department of Environment and Science, GPO Box 2454, Brisbane QLD 4001, Australia

[b] Centre for Green Technology, School of Civil and Environmental Engineering, University of Technology Sydney, P.O. Box 123, Broadway, NSW 2007, Australia

[c] Transport Energy/Emission Research, Brisbane QLD 4001, Australia

* Corresponding author, phone +61 4 6772 1823, fax +61 7 3170 5797, mr.robin.smit@gmail.com

Graphical abstract

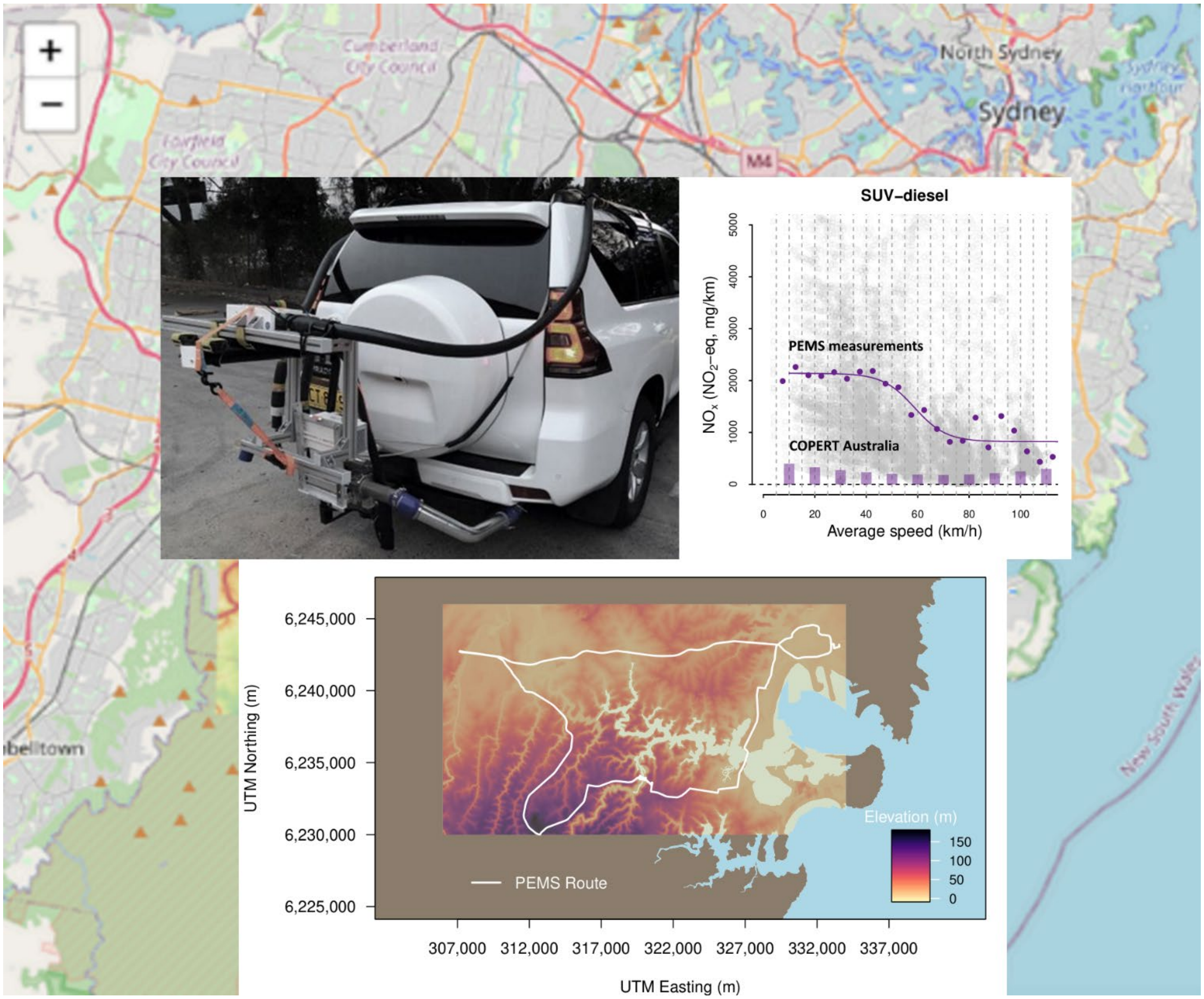

Abstract

Vehicle emissions are a major contributor to ambient air pollution. A variety of techniques are available for quantifying transport emissions for which deployment of a portable emissions measurement system (PEMS) is critical for understanding real-driving fuel consumption and emissions. In this study, we tested the emissions of five sports utility vehicles (SUVs) with a PEMS to address the lack of quality-controlled data in the Australian context. Vehicles were tested for emissions under cold start, hot start and extended idling emissions. The diesel SUV results show that the internationally reported Euro 5 NO_x problem is reproduced in this study with emission factors being on average seven times higher than the type approval limit. Apart from NO_x, the other pollutants measured in this study that includes CO, hydrocarbons, non-methane hydrocarbons and solid particle number are in good agreement with previous international data. Based on the results of this study, COPERT Australia emission algorithms for air pollutants should be revised for more robust estimation of vehicle emissions. On the other hand, COPERT Australia emission algorithms for CO_2 are accurate and do not require an update.

Keywords

Motor vehicle; emission measurement; PEMS; on-board; on-road; emission factors; RDE; real-world

Highlights

- Limited real-driving emissions data exists in the Australian context
- PEMS testing performed on five sports utility vehicles (SUVs)
- Results compared with international studies and COPERT Australia emission algorithms
- Diesel SUVs reproduce the Euro 5 NO_x problem
- Diesel NO_x emissions are seven times the type approval limit

1. Introduction

Exposure to motor vehicle emissions has gained increased interest due to impacts on human health and the environment and associated economic costs (Karner *et al*., 2010; Kimbrough *et al*., 2013). Several studies have linked proximity to busy roads with adverse health effects, including asthma and other respiratory symptoms, birth and development effects, premature mortality, cardiovascular effects and cancer (Baldauf *et al*., 2008; Hood *et al*., 2018). Different methods are used to measure vehicle emissions to quantify their impact on air pollution. They include laboratory chassis and engine dynamometer testing, on-board portable emission measurement system (PEMS), remote sensing, near-road air quality measurements, vehicle chase studies and tunnel studies (Ropkins *et al*., 2009; Smit *et al*., 2010).

Out of the above methods, PEMS plays an important role in vehicle emission model development and generation of emission factors because they enable testing under a wide variety of driving conditions, including traffic density, roadway segment type, road gradients, altitude and environmental conditions (Ntziachristos *et al*., 2016; Zhang *et al*., 2020; McCaffery *et al*., 2020). In particular, on-road PEMS testing overcomes limitations such as poor simulation of resistive loads in chassis and engine dynamometer experiments. Due to these advantages, PEMS have been widely used to measure vehicle gaseous and particulate emissions under real-world conditions.

On-board analysers have been developed since the 1990s, driven by a desire, and later legislative requirements, to measure and quantify real-world fuel use and emissions (Chan *et al*., 1992; André *et al*., 1995; Van Ruymbeke *et al*., 1993; Jetter *et al*., 2000; Dearth *et al*., 2005). PEMS development was initially focussed on heavy-duty vehicles but shifted towards light-duty vehicles in the 2000s (Rubino *et* *al*., 2008). Similarly, PEMS development initially focussed exclusively on emissions of gaseous criteria pollutants, after which the focus shifted to particulate matter (PM) and particulate number (PN) in the 2000s (Giechaskiel *et al*., 2011; Bougher *et al*., 2012; Giechaskiel *et al*., 2015) and NH_3, N_2O and speciated hydrocarbons such as PAHs more recently (Mendoza-Villafuerte *et al*., 2017; Wang *et al*., 2017; Cui *et al*., 2017; Giechaskiel, 2018c; Smit *et al*., 2019; Giechaskiel *et al*., 2019c).

Limited quality-controlled real-driving emissions data exists in the Australian context which we aim to rectify in this study. Although not strictly PEMS studies, Kent *et al*. (1978) and Kent *et al*. (1979) pioneered efforts in Sydney to collect real-driving dynamics data from an instrumented vehicle, followed by chassis dynamometer emissions testing and emissions modelling with a speed-dependent regression technique. More recently, ABMARC (2017) undertook PEMS testing of 30 light-duty vehicles under real-driving conditions in Melbourne, although their data are only available in aggregated form and are not publically available. In the ABMARC study, each vehicle was tested under both cold start and hot start conditions. On average, results suggested a 23 % increase in fuel consumption under real-driving conditions compared to laboratory tests. Furthermore, 13 vehicles exceeded the laboratory type approval limit for NO_x emissions. Given the unique vehicles and fuels used in the Australian fleet further PEMS testing is required to understand transport emissions adequately.

This paper analyses data generated with an on-board measurement campaign that was conducted in Sydney, Australia, with a focus on large passenger vehicles known as Sport Utility Vehicles or SUVs. The Federal Chamber of Automotive Industries (FCAI) defines SUVs as vehicles with a wagon body style and elevated ride height, often with 4WD/AWD capability. This type of vehicle has shown strong growth in vehicle sales in Australia since 2015 (TER, 2019). Due to the increased popularity of SUVs in the

Australian vehicle fleet, in this study we tested five SUVs under real-driving conditions to enable emission factor development and to support assessment of the impact of SUVs on air pollution and greenhouse gas emissions.

2. Methods

2.1 – Test vehicles

Sample selection was based on analysis of Australian vehicle sales and vehicle-specific NEDC-equivalent CO_2 emissions data (TER, 2019). Total vehicle sales and average emission rates were computed over a five-year period (2014 – 2018). Total SUV sales over this period are about 2 million vehicles. The data were subsequently segmented into vehicle technology groups and aggregated to present national sales statistics by brand/model. Vehicles were further classified using the COPERT Australia classification of compact (SUV-C) and large (SUV-L) Sport Utility Vehicles.

To facilitate selection for the test program, mean NEDC CO_2 emission rate was multiplied with total five-year vehicle sales for each selected top 5 brand/model combination to compute a fleet total emission rate (tonne/km). Fleet total emission rates were then summed and used to compute a fleet total emission contribution for each brand/model combination. This statistic is a measure of relative importance of a particular brand/model in terms of CO_2 emission and fuel consumption. It is effectively an emission-weighted sales statistic. Brand/models that have a large contribution are of interest. Table 1 presents an overview of the test vehicle parameters. Four vehicles were hired from commercial rental agencies and one from a car sharing service.

Table 1 – Test vehicle characteristics

Vehicle parameter	VID 1	VID 2	VID 3	VID 4	VID 5
Class	SUV-C	SUV-C	SUV-L	SUV-C	SUV-L
Fuel	Petrol	Petrol	Petrol	Diesel	Diesel
Make	Mazda	Nissan	Toyota	Isuzu	Toyota
Model	CX-5	X-Trail	Kluger	MU-X	Prado
Year of manufacture	2015	2020	2019	2018	2019
Emission standard	Euro 5	Euro 5	Euro 5	Euro 5	Euro 5
GVM (kg)	2175	2205	2760	2750	2990
Test weight (kg)	2100	2045	2500	2700	2940
Engine capacity (l)	2.5	2.5	3.5	3.0	2.8
Number cylinders	4	4	6	4	6
Rated power (kW @ rpm)	138 @ 6000	126 @ 6000	218 @ 6600	130 @ 3600	130 @ 3400
Transmission	Automatic	Automatic	Automatic	Automatic	Automatic
Number gears	6	6	8	6	6
Wheels driven	4WD	4WD [1)]	4WD	4WD	4WD

[1)] Although this vehicle is listed as high volume 4WD in vehicle sales data, the vehicle manufacturer advised this is in fact a 2WD vehicle.

*2.2 – Test equipment **and protocols***

Testing deployed an AVL 493 Gas PEMS iX, an AVL 496 PN PEMS and a 2.5-inch AVL 495 exhaust flow meter designed for light duty vehicles. Ambient conditions (temperature, relative humidity and atmospheric pressure) were measured with a meteorological sensor. A GPS unit (Garmin GPS 16x, WAAS compatible) was used to collect locational latitude (LAT), longitude (LON), elevation and speed data. Elevation data from the GPS was found to be of lower quality compared to data from a Digital Elevation Model (see section 3.3) and hence was not used in this study. Electronic Control Unit (ECU) data were collected through the On-Board Diagnostics (OBD) port using a Dearborn DPZ5 OBD II scanning tool. A video camera (XCD ELS1 dash cam, 720P resolution, 30 F) was installed on the dashboard to enable analysis of specific parts of the trip at a later stage. A range of exhaust pollutants were measured at 10 Hz including CO_2, CO, NO, NO_2, solid PN (SPN), methane (CH_4), non-methane hydrocarbons (NMHC) and oxygen (O_2). Fuel consumption was estimated with a carbon mass-balance approach for all tests, although fuel consumption data were available from the OBD II port for one vehicle as well. Physical installation of the PEMS in each test vehicle followed the guidelines presented by Giechaskiel *et al*. (2016). A linearity check on the Gas PEMS was performed before the start of the experimental campaign. **Pre-tests for each PEMS test involved performing a system purge and leakcheck, followed by zero and span calibrations as well as zeroing of the exhaust flow meter. A system purge followed by zero and span drift checks were performed after each PEMS test.**

2.3 – Test protocol and routes

The on-road test program included a cold start test, which is defined as a soak of at least 12 hours, three warm start tests, an extended idle test of at least 10 minutes, as well as a coast-down test and fuel quality test. A detailed overview of the test protocol is included in the Supplementary Material (SM1).

A PEMS cold start test route was initially developed at UTS for Sydney with guidance from AVL engineers. It reflects real-world driving conditions in the Sydney metropolitan area and includes urban (24.8 km), rural (26.1) and freeway (19.4) driving conditions, spanning a range of driving speeds from 0 to 100 km/h. After initial testing, the length of the motorway segment was increased to make the motorway segment RDE compliant in terms of length and duration. A steep road gradient section was also added to capture high power events on hilly roads. Overall, RDE compliance was achieved with the test route in some tests, but it was generally difficult to achieve the required motorway distance and time shares on the M5 motorway travelling eastbound.

A second shorter 'residential' test route was developed to specifically test for warm start emissions. The warm start test sequence continued after completion of the cold start PEMS test and after recharging of the battery (about 2 hours). The time intervals with the engine off before restart were approximately two hours, and then 5, 15 and 30 minutes, respectively. In terms of vehicle operation during the test, all vehicles operated with windows closed, air-conditioning on (target temperature 23°C, moderate fan speed), heating off, seat warming off, radio off and lights on. Finally, a coast-down test was conducted for each vehicle (refer to section 2.6).

2.4 Pre-test protocols

After hiring each vehicle, a wheel alignment was performed by a local mechanic. This was followed by setting tyre pressures at 3 psi below the manufacturer-recommended maximum tyre pressure. After this, a local mechanic drained the fuel tank and refilled each vehicle from a batch of either petrol or diesel fuel for which fuel quality parameters are known (Table 2). Petrol vehicles were re-fuelled with 35 litres from the batch of petrol fuel and diesel vehicles with 45 litres from the batch of diesel fuel.

2.5 – Fuel quality

Test vehicles used commercially available fuel at the bowser. Previous research has shown that a unique fuel quality situation exists in Australia (Smit *et al*., 2021). For several legislated fuel parameters, Australian and European Union (EU) fuel quality standards and the quality of in-use diesel and petrol fuels are the same or, at least, similar. The main differences relate to specific petrol fuel parameters such as MTBE, MON/RON, sulfur, and fuel volatility. A batch of diesel and petrol fuel were stored for the duration of the test program. A fuel sample analysis was performed to determine fuel quality. A detailed overview of the fuel quality testing results is included in the Supplementary Material (SM2). A selection of fuel parameters is shown in Table 2.

Table 2 – Fuel quality testing results for selected fuel parameters

Petrol fuel parameter	Test result	Diesel fuel parameter	Test result
RON	92	Cetane index	54
Total Saturates	62 % v/v	PAH content	3 % m/m
Total Aromatics	26 % v/v	Total Aromatics	24 % m/m
Total Olefins	12 % v/v	Density	0.83 kg/l
Total Oxygenates	0.07 % m/m	FAME	< 0.05 % v/v
DVPE	59.7 kPa	Ash content	< 0.01 % m/m
Sulfur content	11 mg/kg	Sulfur content	9 mg/kg

2.6 – Coast down testing

Coast-down tests were performed to enable estimates of rolling resistance and aerodynamic drag coefficient in the road load force equation to be made. Coast-down testing was guided by the principles of SAE J1263 (2010) for which some items of the test procedure where compliant with the standard and others not. The main complication involved finding a suitable road to safely facilitate coast-down testing with PEMS instrumentation fitted to a vehicle. While a solution was found at the Nirimba Education Precinct, the length of the test track was 575 metres, which forced some engineering judgements to be applied. In particular, the maximum speed that could be safely achieved was 70 km/h and coast-down runs could only be run in one direction due to the unevenness of the road surface on the western edge of the test track. In addition, coast-down timing resolution of 0.5 seconds was achieved instead of the 0.1 seconds recommended by SAE J1263. On the other hand, accuracy and resolution of the test equipment for speed measurement and measurement of meteorological parameters with a weather station (Davis Instruments, USA) including wind speed, wind direction, temperature and barometric pressure were compliant with SAE J1263.

Velocity versus time data from coastdown tests were analysed using the method of White and Korst (1972) as recommended by SAE J1263. Non-dimensionalisation was performed on the raw velocity versus time data which yielded a non-dimensionalised family of curves represented by the parameter $\boldsymbol{\beta}$ via:

$$\boldsymbol{\nu} = \frac{\boldsymbol{v}}{\boldsymbol{v_0}} = \frac{\mathbf{1}}{\boldsymbol{\beta}}[\mathbf{tan}(\mathbf{1}-\boldsymbol{\tau})\,\mathbf{tan}^{-\mathbf{1}}(\boldsymbol{\beta}) + \boldsymbol{\tau}\mathbf{tan}^{-\mathbf{1}}(\boldsymbol{\kappa}\boldsymbol{\beta})]. \quad (1)$$

Since the final coastdown speed (v_f) was non-zero, the method of White and Korst yielded an additional integration constant $\boldsymbol{\kappa} = \frac{\boldsymbol{v_f}}{\boldsymbol{v_0}}$, while v represents non-dimensionalised speed, v_0 is the initial coastdown speed and τ is non-dimensionalised time. A Gauss-Newton method available in the non-linear least squares (nls) function in R was used to estimate β in equation 1.

After β was approximated, the rolling resistance (R) was estimated using:

$$\boldsymbol{R} = \frac{\boldsymbol{m_{eff} v_0}}{\boldsymbol{\beta g t_0}} [\mathbf{tan^{-1}}(\boldsymbol{\beta}) - \mathbf{tan^{-1}}(\boldsymbol{\kappa\beta})],$$

while the aerodynamic drag coefficient (C_d) was estimated using:

$$\boldsymbol{c_d} = \frac{\mathbf{2}\boldsymbol{m_{eff}\beta}}{\boldsymbol{\rho A v_0 t_0}} [\mathbf{tan^{-1}}(\boldsymbol{\beta}) - \mathbf{tan^{-1}}(\boldsymbol{\kappa\beta})],$$

where m_{eff} is the effective mass of the vehicle, ρ is the density of air, A is the frontal area of the vehicle, t_0 is the total coastdown time and g is the acceleration due to gravity. An example of the fitting procedure for coastdown data is provided in Figure 1, while tabulated results for coastdown testing are shown in SM3.

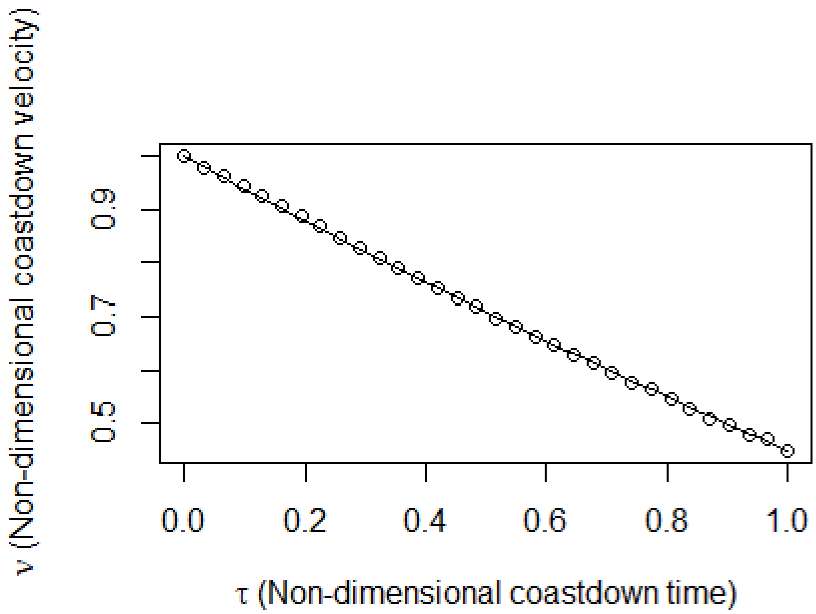

Figure 1 – Example fit of non-dimensionalised velocity versus time coastdown data for VID 1. For this fit β=0.58725.

3. Theory and calculation

3.1 – Data post-processing

AVL's post-processing tool Concerto was used to time-align all relevant signals. AVL Concerto uses a combination of measured time offsets and a pairwise correlation technique to align all signals to the point of measurement that is overviewed in Supplementary Material (SM11).

NO emissions were converted to NO_2-equivalents (molar mass ratio of 1.53) to compute NO_x emissions expressed as NO_2-equivalents.

Fuel consumption was computed using the carbon-balance approach as per ECE Regulation 101 (12 April 2013), which uses measured CO, HC and CO_2 emission rates as inputs.

3.2 – Speed and acceleration data

Recorded GPS and OBD speeds were processed and verified (Smit, 2013b). All recorded OBD and GPS speeds less than 0.5 km/h and 1.0 km/h were set to zero, respectively. Speed-time traces were visually checked to identify and rectify any periods with GPS and/or OBD signal loss. The GPS data were used to estimate vehicle speeds, except for driving inside the tunnel where OBD speeds were used (refer to section 3.3). Missing speed values in the final speed traces were imputed using cubic spline interpolation. A three-pass T4253H filter (Velleman, 1980; Smit, 2013a) was applied to the speed traces to account for measurement noise and to prevent unrealistic computations of acceleration and engine power, particularly at higher speeds.

Acceleration was computed using speed changes over 2-3 second intervals (Smit, 2013b). Speed-dependent 'maximum feasible acceleration' functions were then used to flag any potentially unrealistic accelerations in the PEMS data. These reverse sigmoid functions (plus an error margin of 30%) were developed for different rated power-to-weight ratios (Katsis *et al*., 2016). The speed - acceleration data exhibits realistic behaviour for each vehicle (Supplementary Material SM4).

3.3 – Road gradient

Road gradient can significantly impact fuel consumption and emissions (Frey *et al*., 2008; Boriboonsomsin *et al*., 2009). Compared with flat roads, steep road gradients (≥ +5%) can lead to substantial emission increases in the order of a factor of two to six for individual vehicles, or even significantly higher (Fontaras et al., 2017; Gallus *et al*., 2017). It is therefore important that road gradient information is included and considered in the development of emission factors.

High accuracy elevation data are required for the computation of road gradient at a high resolution of 1 Hz. Elevation data were collected with the GPS or can be extracted from external data sources in a post-processing step, such as near-global NASA Shuttle Radar Topography Mission (SRTM), which represents height in meters above sea level (elevation) with the WGS84 coordinate reference system (CRS) (Lovelace *et al.*, 2019), or local Digital Elevation Models (DEMs). The local Elevation Information System (Geoscience Australia, 2021) is a 1-meter Digital Elevation Model (DEM). It was used in this study as it has the highest resolution (1 m) and provides the most accurate elevation data (Figure 2).

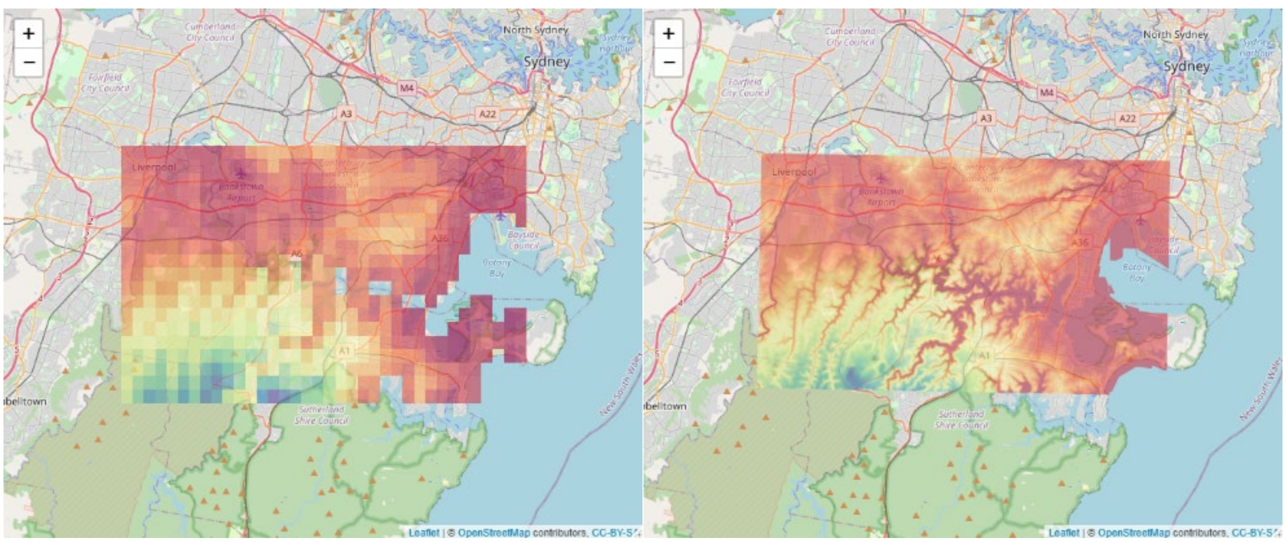

Figure 2 – R Leaflet Maps visualizing the resolution of STRM data (left) and local DEM data (right) for the study area.

The DEM is produced using the Triangular Irregular Network method of averaging ground heights to create a regular grid. This data set contains ground surface information in an ASCII grid format derived from LiDAR (Light Detection and Ranging) from an Airborne Laser Scanner. The 1 m DEM has a vertical accuracy of 15 cm and a horizontal accuracy of 45 cm in most areas. R studio version 1.3.1058 (R Studio

Team, 2015) and R version 4.0.2 (R Core Team, 2017) were deployed to extract elevation data for the area of interest. The raster data were stored as a TIF file.

GPS LAT/LON trip coordinates (1 Hz) were extracted from each vehicle test and converted into spatial vector data (KML and CSV files). The raster library in R was then deployed to extract elevation data from the 1 m DEM raster file at all coordinates in the spatial vector data. For each location, the mean elevation was computed for a buffer with a radius of 10 m. WGS 84 was used as the geographic CRS for all data, but for visualisation the spatial data were projected to Universal Transverse Mercator: UTM 56S (Figure 3).

The elevation estimates using the 1 m DEM were compared with separate estimates made using elevation provided by the GPS directly and STRM data (refer to Supplementary Material SM5 for examples). The analysis showed that STRM provides elevation data that is too coarse at 1 Hz, whereas GPS altitude data appear to be prone to drift and occassional signal loss.

Road gradient (%) was computed with 100 TAN(ASIN($\Delta h/v$), where Δh is the difference in elevation between time = t+1 and time = t and v is the average speed in this two-second time period. A (moving average, $\alpha = 3$) linear filter was applied to the elevation data to smooth out sudden fluctuations. Road gradient is automatically set to zero degrees at instantaneous speeds below 2 km/h to prevent computation of unrealistically large road gradients that are at low speeds. Any road gradient values between -0.25% and +0.25% are set to zero to eliminate residual noise in the road gradient profile.

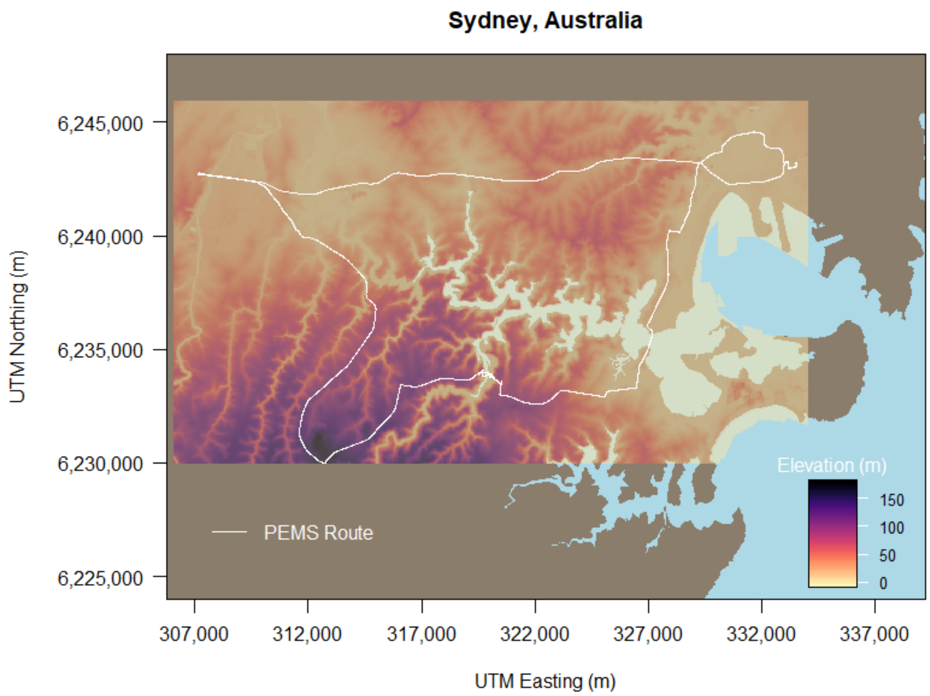

Figure 3 – UTM Map (56S) showing the route taken during PEMS measurements in Sydney and the external elevation data provided by the 1 m DEM Elevation Information System.

3.4 – Tunnel data

A small portion of the on-road test passes through the M5 East tunnel (3-4 minutes; about 4 km) with an associated loss of GPS signals involving speed, location and elevation. To rectify this, information on tunnel geometry was obtained from Transport for New South Wales. This information was used to reconstruct a tunnel elevation profile with a 1 m resolution, which extends from tunnel entry to 200 m after tunnel exit. The 200 m extension accounts for the time delay needed for GPS signals to accurately record position. R (sf library) was used to identify the nearest LAT/LON coordinate to either the tunnel entry or tunnel exit (+ 200 m) location in each emission test. Recorded vehicle OBD speed was then used to cumulatively determine the distance, exact location and associated elevation inside the tunnel from tunnel entry onwards.

Tunnel design data could not be obtained for a shorter second tunnel (Cooks tunnel, about 500 m). The time at tunnel entry and 200 m after tunnel exit were determined and flagged for removal in the PEMS database. The time between these points takes about 35 seconds to traverse.

3.5 – Power and work

On-road engine power was estimated using PΔP model algorithms (Smit, 2013; 2014), which consider aerodynamic resistance, tyre rolling resistance, drive train/transmission resistance, inertial resistance, gravitational resistance and use of auxiliaries. The model structure is briefly described in the Supplementary Material (SM6). The input to the PΔP power prediction algorithms is speed-time data and road gradient data (1 Hz) and information on vehicle loading and use of air conditioning (i.e. on/off). Power estimates were used to compute accumulated positive work for each second since engine start or restart.

A strong correlation should exist between instantaneous positive engine power and fuel consumption rate for quality-controlled emissions data (Smit, R., 2013b; Katsis *et al*., 2016). The correlation can be distorted by regeneration events of the diesel particulate filter (DPF) and auxiliary engine strategies as well as data quality issues such as sensor glitches, incorrect time alignment, inaccurate road gradient information and inaccurate vehicle parameters. To verify the computed power values, the Pearson correlation coefficient between fuel consumption and simulated positive engine power was computed for each test. The results varied between 0.72 and 0.94, with an average value of 0.86, which is within the expected range for on-road tests.

The power distributions were also checked visually by 1) plotting power versus speed including rated engine power, 2) power distributions (histogram) and 3) CO_2 emission engine maps showing binned normalised power versus normalised engine speed. Rated engine power is an indicative real-world maximum value for estimated power. An exceedance of 10% of rated engine power is considered acceptable. The visual assessment of power distributions and CO_2 emission engine maps confirmed that estimated power is generally realistic and behaves as expected. An example is shown in Figure 4 (refer to Supplementary Material SM7 for **the** complete set).

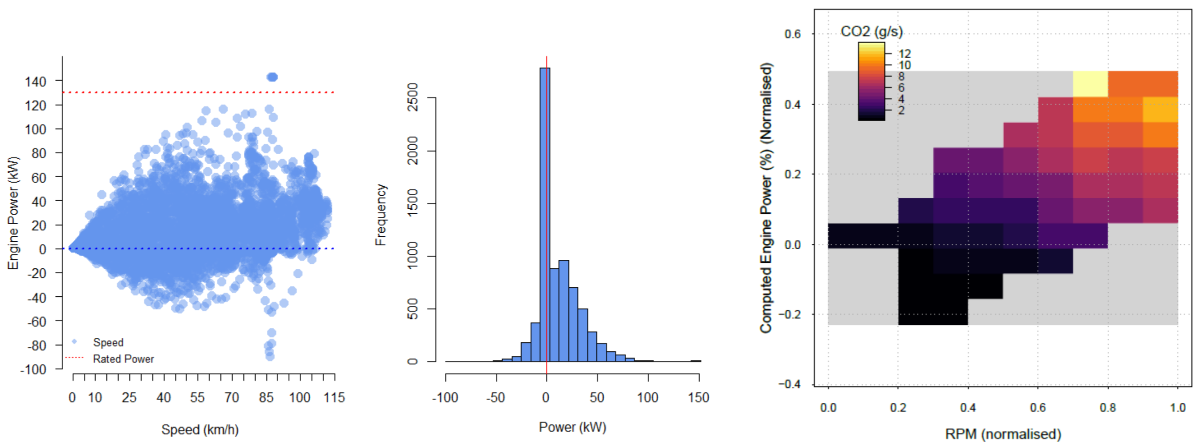

Figure 4 – Examples of (left) computed engine power versus speed, (middle) power distribution, (right) engine CO_2 emission maps.

3.6 – RDE compliance

The purpose of the study was explicitly to develop real-world emission factors for Australian SUVs. The tests were generally in compliance with RDE requirements. Based on the four RDE packages issued thus far, the tests are non-compliant for the following items:

1. Trip shares in terms of time and distance for the motorway section were non-compliant apart from testing for one vehicle.
2. A motorway segment involving speeds > 100 km/h for five minutes could not be achieved due to the enforced speed limit of 100 km/h.
3. Weekend testing was involved.
4. Data interruptions of > 30 seconds occurred due to sensor malfunctions of the NDIR for VID 1.
5. None of the vehicles for which coolant temperature data were available achieved a cold start duration of five minutes or less.
6. GPS interruptions exceeded 120 seconds due to travelling through the M5 tunnel.

3.7 – Engine start emission factors

After a significant soak period[1], the vehicle engine and emission control systems are typically cold (ambient temperature), which means additional fuel is required and emission control efficiency is reduced. When vehicle engine, transmission and emission control technologies are operating at normal operating temperatures (engine coolant 70-90 °C, catalysts > 200-250 °C), they are in hot running conditions. Hot running conditions are generally achieved for all relevant vehicle components (engine, transmission, emission control system) within 15 minutes of driving. However, the magnitude of additional start emissions is largely determined by light-off conditions for the catalyst systems and tight control of the air-to-fuel ratio, which are typically achieved rapidly and within a minute of engine start

[1] From a practical point of view approximately > 1 hour (Zachariadis 1999), but at least 12-36 hours from a legal emission standard testing perspective (Appel 2021).

for modern vehicles (Smit and Kingston, 2019). Vehicle emissions are significantly elevated in engine start conditions, and particularly in cold start conditions. The magnitude of hot or warm start emissions[2] depends on how long the vehicle has been turned off, but emissions are lower than cold starts.

Cold start emission factors require determination of either the cold start distance or the cold start period needs to be determined. Phase detection functions have been previously to determine the points in time and space where the cold start period ends (Favez *et al*., 2009; Smit and Ntziachristos, 2013). For PEMS studies, the determination of cold start periods is simply defined by a cold start period of 5 minutes (Weiss et al., 2011b; Bielaczyc et al., 2020) or a cold start distance of 10 km (Kousoulidou, 2013). The European Commission (EC, 2018) defines an RDE cold start as the period from the test start until the point when the vehicle has run for 5 minutes. Alternatively, if the coolant temperature is measured, the cold start period ends once the coolant reaches 70°C for the first time, but no later than 5 minutes after test start. An RDE hot start is defined as an engine start with a warm engine with engine coolant temperature and/or engine oil temperature above 70°C.

In this study coolant temperatures were measured continuously by the OBD systems, except for VID 4 where coolant temperature is not available. For the cold start tests, the time periods from engine start until 70°C coolant temperature were determined (except for VID 4). Using this method ("70°C"), cold start periods varied from about 4 to almost 7 minutes, reflecting vehicle-specific differences in emission control technology, engine calibration and cold start emission management, as well as

[2] Hot starts were traditionally defined as a start after a ten-minute soak time in the US FTP 75 test procedure (NRC, 2000).

variation in ambient conditions and driving conditions (e.g. congestion, road gradient and presence of traffic lights during the cold start trip).

For VID 4, accumulated positive engine work since engine start (W^{+}_{acc}) was used to determine the cold start period (Wong *et al*., 2019). W^{+}_{acc} was computed for the end of the cold start period for each vehicle with OBD data and divided by vehicle test weight to normalise for differences in energy requirements and reduce the coefficient of variation (COV). On average, 0.40 kWh/tonne (COV = 22%) of accumulated positive engine work is required to reach an engine coolant temperature of 70°C. This threshold was used to determine the cold start period for VID 4, estimating a cold start period 5:13 and 5:41 minutes for the two cold start tests.

The hot start tests (approximately 10-minute duration) took place after different engine-off soak periods ranging from a few hours, then 5 minutes, 15 minutes and 30 minutes. The tests with 5-to-30 minutes soak times experienced engine coolant temperatures above 70°C throughout the tests (81-93°C). The first hot start sequence (after a few hours soak) started at lower coolant temperatures, varying between 41 and 61°C, and the "70°C" method was applied.

Total start emissions were computed for each vehicle for different soak periods (5, 15 and 30 minutes, about 2 hours, cold start) by summing emissions until the vehicle-specific W^{+}_{acc} value was reached during both the cold and hot start tests. The 5-minute soak period was considered to approximate hot running emissions and taken as the baseline emission value. This baseline value was subtracted from total emissions for the other soak periods to compute start emissions (g/engine start). A detailed overview of the results is included in the Supplementary Material (SM8).

3.8 – Urban, Rural and Motorway emission factors (hot running)

Second-by-second speed data were used to allocate the urban, rural and motorway road types using speed criteria defined in Commission Regulation 2017/1151 (EC, 2017). Clauses 6.3 to 6.5 define urban operation as (SUV) vehicle speeds (v) ≤ 60 km/h, rural operation as 60 < v ≤ 90 km/h and motorway operation as v > 90 km/h. These criteria were applied to all vehicle test data for each vehicle combined, but excluding the cold start period, to split the data into urban, rural and motorway conditions.

A bootstrap analysis was conducted to estimate the grand mean and associated standard error and non-symmetric 95 percent confidence intervals (95% CI) for each vehicle, pollutant and road type. The bootstrap resamples the data with replacement and the estimate is calculated for this new resampled data set. This is repeated many times to form an approximate sampling distribution for the estimate, from which standard errors and confidence intervals can be calculated (James *et al*., 2017).

3.9 – Manoeuvre-based emission factors (hot running average speed)

An alternative approach to emission factor development is a manoeuvre-based approach which splits the PEMS data and creates driving segments of prespecified length, which are subsequently used as an input for statistical modelling. This automated procedure was developed for the development of hot running emission factor algorithms for the COPERT Australia software (Smit and Ntziachristos, 2012), as shown in Figure 5. It shows five micro-trips ('stop-go-stop' driving patterns) in the top chart, denoted with A, B, C, D and E. The procedure first tags each second of PEMS data as idling, start, move or end, following a set of speed-related allocation rules. Three types of driving segments of a length of 500 m are then extracted from the "move" speed-emissions data for each micro-trip, a) driving segments that start with an acceleration (starting point of a micro-trip), b) driving segments that end with a deceleration (end point of a micro-trip), and c) 'snippets', which are created by moving through the micro-trip, each time creating a new PEMS data extract of approximately 500 m driving distance. Figure 5 shows the three types of segments for micro-trip D with a grey shading area.

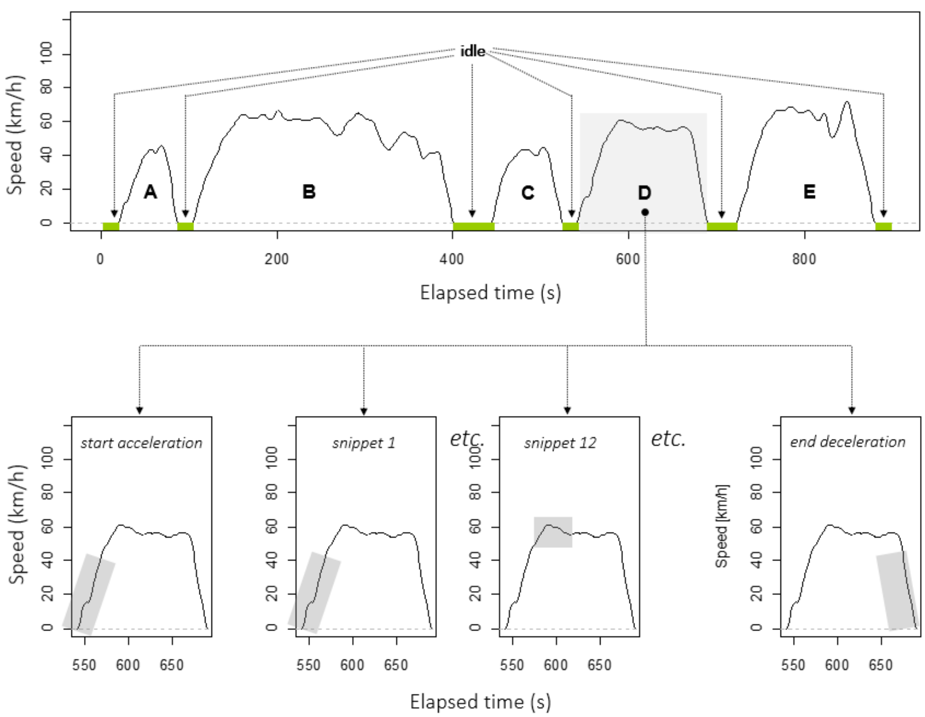

Figure 5 – Schematic of PEMS segmented database creation (Source: Smit and Ntziachristos, 2012).

Idle segments are then combined with ‘start acceleration’ as well as all ‘end deceleration’ segments on the condition that the difference in coolant temperature is less than 10°C to ensure consistency in engine and emission control operational conditions. This procedure creates a database from individual PEMS measurements that contains three types of driving manoeuvres: a) idle-acceleration, b) deceleration-idle and c) moving vehicle without stops and idling periods and at different running speeds. For each manoeuvre, distance and time information are determined, and emission factors and average speed are computed for all pollutants. Processing the SUV PEMS data this way generated a database with 42,002 emission factors for five vehicles.

Hot running emission factors were extracted using manoeuvres with an average engine coolant temperature above 70°C. As discussed before, VID 4 (MU-X) did not retrieve OBD coolant temperature data. A further analysis of the relationship between exhaust gas temperature and engine coolant temperature for the other vehicles, showed a weak to moderate correlation (Pearson correlation coefficient varying from 0.21 to 0.59). The point where coolant temperature first reached 70°C corresponded (on average) to exhaust gas temperatures of about 70°C for the warm start and 115°C for the cold start. The combination of exhaust gas temperature and these threshold values were used as a proxy for identifying segmented hot running emission factors for VID 4.

The empirical (manoeuvre-based) emission factor database was used to develop emission factor algorithms following the approach used for COPERT (Samaras and Geivanidis, 2005). The test vehicles were allocated to the corresponding (Euro 5) COPERT Australia vehicle class, i.e. compact petrol SUV (VID 1 and 2), large petrol SUV (VID 3) and diesel SUV (VID 4 and 5). The cold start and hot start test data for the individual vehicles were pooled according to vehicle class. Mean emission factors were computed for 26 speed bins (5 km/h increments) to avoid overweighting of specific speed intervals with a high number of data points. The average emission factor values for each per bin represent the arithmetic mean of all manoeuvre-based emission factors that fall within the speed bin. A non-linear least-squares regression was applied to the binned average emission factor values to fit the data to the generic polynomial COPERT emission factor function: $EF = (a + b\nu + c\nu^2)/(1 + d\nu + e\nu^2) + (f/\nu)$, where ν represents the average bin speed (km/h) and $a - f$ represent the fitted model coefficients. Simplified versions of the generic COPERT emission factor function and logistic regression functions were also included. The Akaike Information Criterion (AIC) criterion was used to select the best algorithm (James *et al*., 2017). AIC estimates the quality of each model fit, relative to each of the other candidate models. AIC rewards goodness of fit but includes a penalty for the number of estimated model parameters.

The fitted emission factor algorithms were then compared with hot running emission factors used in the latest version of COPERT Australia (v1.3.5).

3.10 – Extended idling

Idling is defined as running the engine when the vehicle is stationary (TER, 2020). Idling occurs regularly while driving in real-world conditions (for instance waiting at traffic lights). Survey data in Europe, North America and Australia show that (in-traffic) idling typically accounts for 13% - 23% of vehicle travel time (Dong *et al*., 2014; TER, 2020). Another type of idling occurs when leaving the engine on while parked, either out of habit or to provide services unrelated to driving, such as cooling or heating the cabin. California's anti-idling regulations define excessive idling as a long and unnecessary idling period 5 minutes or longer while parked (Lust *et al*., 2008). Idle engine operation is inefficient and involves incomplete combustion, resulting in increased fuel consumption and elevated emissions (Shancita *et al*., 2014).

Limited research has been published on the net emission effect for modern vehicles of excess restart emissions versus avoided emissions due to engine shutdown (Calcagno, 2005; Dong *et al*., 2014). A research study in the Netherlands (TNO, 2005) measured idling emissions from diesel and petrol cars (Euro 3 and 4) after 1-, 2- and 5-minute engine stop intervals. The measurements show that an engine shut down reduces emissions for short stops for CO_2 (all cars), NO_x and PM (diesel cars), but that idling may be beneficial for NO_x, CO and VOC emissions (petrol cars) due to the prevention of catalyst cooling. For long stops (more than one hour) engine shut down is always beneficial.

This study included emissions testing in extended idling conditions of approximately 10 minutes duration. In addition, warm start emissions were determined after a 15-minute soak period in this study (Table SM8.3). These emission rates (g/start) are compared with cumulative idling emissions to examine the net emissions effect of re-start versus extended idling. The point in time where cumulative idling emissions equal additional restart emissions have been determined, whenever possible. Idling after this point in time will increase net emissions. When either start or cumulative idling emissions are negative, this point could not be determined. Negative emissions are considered to generally represent very low and negligible emission rates close to the detection limit of the test equipment.

Regarding assessment of non-constant emissions behaviour over time, a statistical test was applied to the time-series data to investigate whether a structural change in the linear regression relationship can be detected (Zeileis *et al*., 2002). Using the F statistic and the weighted average criterion expF (Andrews and Ploeberger, 1994), a p-value < 0.05 provides evidence for the alternative hypothesis (structural change) over the null hypothesis (no structural change).

4. Results and discussion

This section presents the exhaust emission factors derived from the PEMS data following the methods discussed in the previous section and include engine start, road type hot running (i.e. urban, rural, motorway), average speed hot running (micro-trips) and extended idling.

4.1 – Engine start emission factors

Table 3 (cold start) and 4 (hot start) show the results for selected pollutants. Cold start emissions for petrol SUVs are significantly higher than diesel SUVs for CO, HC and PN. However, excess NO_x emissions due to cold starts are significantly higher for diesel vehicles. Of interest are the results for the two cold start tests with the Toyota Prado. The tests were conducted in relatively warm (27°C) and cold (17°C) ambient conditions. The colder test had a longer cold start period (407 versus 315 seconds), a longer cold start distance (4.6 km versus 1.4 km) and double the amount of engine work required to achieve hot running conditions (1.6 vs. 0.8 kWh). Cold start emissions are significantly elevated as a result.

Hot start emission factors for a 30-minute soak (Table 4) show that start emission factors are generally substantially lower than cold start emission factors, as would be expected. For several vehicles and pollutants, the start emission factors are close to zero or even negative.

As an alternative method, a fixed 5-minute cold start period was assumed for all vehicles. The 5-minute start period was also applied to all hot start sequences. As a first step average emission factors (g/km) were computed for all vehicles and all tests using the first 5 minutes of data for each emission test. These emission factors were then multiplied with the vehicle-specific cold start distance, which varied from 2.5 to 3.8 km, to compute the engine start emission factor (g/start). Table SM8.1 (cold start) and SM8.2 (hot start) show the detailed results for selected pollutants.

Table 3 – Cold start emission factors

SUV VID (P = petrol, D = Diesel,	Mean ambient temperature during cold	Accumulated positive engine work	Cold start emission factors (g/start or #/start)			
			CO	THC	NO_x (NO_2-eq)	PN ($\times10^{11}$)

C = Compact SUV, L = Large SUV)	start test (° C)	W^{+}_{acc} (kWh/t)				
VID 1 (C, P)	24	0.33	9.99	1.13	1.32	175.34
VID 2 (C, P)	25	0.35	4.97	0.49	0.63	143.06
VID 3 (L, P)	19	0.47	11.29	0.63	0.12	330.39
VID 4 (C, D)	20	0.40	0.20	0.03	7.48	83.43
VID 5 (L, D)	22	0.41	0.12	0.07	5.30	10.17

A comparison shows that the two approaches to estimate cold start emission factors produce generally similar results (refer to Figures SM8.1 and SM8.2). The results can vary significantly for specific combinations of vehicle and pollutant, particularly for small start emission factors. However, at an aggregated level the results are reasonably robust. For petrol SUVs, the W^{+}_{acc} method produces mean cold start emission factors that are 4% (CO), 16% (THC), 30% (NO_x) and 0.4% (PN) higher than the 5-minute method. For diesel SUVs, the W^{+}_{acc} method produces mean cold start emission factors that are 29% (CO), 33% (THC), 21% (NO_x) and 10% (PN) lower than the 5-minute method. It is expected that the W^{+}_{acc} method produces more accurate results as emissions data are normalised for variability in driving conditions (for instance congestion and road gradient) that is inevitably encountered during on-road emission testing. To be conservative, the 5-minute method could be used for diesel vehicles.

Table 4 – Hot start emission factors (30-minute soak period)

SUV VID	Mean	Accumulated	Warm start emission factors			
(P = petrol, D = Diesel,	ambient temperature during warm	positive engine work	CO (g/start)	THC (g/start)	NO_x (NO_2-eq) (g/start)	PN ($\times 10^{11}$) (#/start)

C = Compact SUV, L = Large SUV)	start test (° C)	W^{+}_{acc} (kWh/t)				
VID 1 (C, P)	21	0.33	9.54	0.23	0.30	-9.42
VID 2 (C, P)	23	0.35	-0.95	0.01	0.22	-2.54
VID 3 (L, P)	18	0.47	0.83	0.05	-0.02	-11.30
VID 4 (C, D)	18	0.40	-0.05	0.00	-0.90	-2.50
VID 5 (L, D)	22	0.41	-0.06	0.00	-0.27	-0.01

4.2 – Urban, Rural and Motorway emission factors (hot running)

Table 5 shows the road type specific hot running emission factors for the individual vehicles.

Table 5 – Hot running SUV emission factors by vehicle, pollutant and road type (bootstrap mean ± standard error)

	CO_2 (g/km)			NO_x (mg/km)			NO_2 (mg/km)		
VEHICLE ID *	URB	RUR	MWY	URB	RUR	MWY	URB	RUR	MWY
VID 1 (C, P)	303 ± 5.5	155 ± 3.6	63 ± 7.4	60 ± 3.5	28 ± 2.7	17 ± 1.5	5 ± 0.1	2 ± 0.0	2 ± 0.1
VID 2 (C, P)	315 ± 4.8	148 ± 2.7	147 ± 2.4	69 ± 3.2	26 ± 1.3	17 ± 1.5	8 ± 0.1	4 ± 0.1	3 ± 0.1
VID 3 (L, P)	388 ± 5.9	184 ± 4.2	172 ± 4.8	24 ± 0.8	13 ± 2.0	16 ± 3.2	5 ± 0.1	2 ± 0.0	2 ± 0.0
VID 4 (C, D)	334 ± 4.3	174 ± 2.4	176 ± 2.4	2497 ± 66.9	913 ± 33.4	691 ± 32.0	312 ± 5.8	134 ± 3.4	115 ± 3.9
VID 5 (L, D)	377 ± 4.3	196 ± 2.9	212 ± 2.9	2002 ± 44.2	970 ± 34.5	749 ± 29.4	357 ± 7.2	207 ± 6.1	181 ± 6.6

	CO (mg/km)			THC (mg/km)			PN (10^{11} #/km)		
VEHICLE ID *	URB	RUR	MWY	URB	RUR	MWY	URB	RUR	MWY
VID 1 (C, P)	2575 ± 282.1	1650 ± 342.5	49 ± 6.0	53 ± 3.8	22 ± 2.8	13 ± 0.9	14.06 ± 0.570	7.24 ± 0.405	2.64 ± 0.379
VID 2 (C, P)	3772 ± 453.7	1433 ± 210.3	624 ± 46.4	29 ± 1.4	10 ± 0.6	10 ± 0.4	5.93 ± 0.370	3.77 ± 0.252	1.49 ± 0.200

VID 3 (L, P)	1524 ± 302.6	725 ± 278.5	38 ± 3.4	13 ± 1.3	2 ± 0.3	-1 ± 0.2	8.86 ± 0.910	7.00 ± 0.873	2.64 ± 0.266
VID 4 (C, D)	-43 ± 0.5	-20 ± 0.2	-18 ± 0.3	15 ± 0.6	4 ± 0.2	2 ± 0.0	4.60 ± 0.458	0.05 ± 0.005	0.01 ± 0.001
VID 5 (L, D)	-34 ± 0.5	-21 ± 0.3	-24 ± 0.4	9 ± 0.2	3 ± 0.1	2 ± 0.0	5.91 ± 0.511	1.34 ± 0.299	0.01 ± 0.000
	CH_4 (mg/km)			NMHC (mg/km)			NO (mg/km)		
VEHICLE ID *	URB	RUR	MWY	URB	RUR	MWY	URB	RUR	MWY
VID 1 (C, P)	1.2 ± 0.09	0.5 ± 0.07	0.3 ± 0.02	52 ± 3.9	22 ± 2.9	13 ± 0.8	36 ± 2.3	17 ± 1.8	9 ± 1.0
VID 2 (C, P)	0.7 ± 0.03	0.2 ± 0.01	0.2 ± 0.01	28 ± 1.4	10 ± 0.6	10 ± 0.4	40 ± 2.1	14 ± 0.8	9 ± 0.9
VID 3 (L, P)	0.3 ± 0.03	0.0 ± 0.01	0.0 ± 0.01	13 ± 1.3	1 ± 0.3	-1 ± 0.2	12 ± 0.5	7 ± 1.3	10 ± 2.0
VID 4 (C, D)	0.3 ± 0.01	0.1 ± 0.01	0.0 ± 0.00	14 ± 0.5	4 ± 0.2	2 ± 0.0	1424 ± 36.9	508 ± 19.7	376 ± 18.5
VID 5 (L, D)	0.2 ± 0.00	0.1 ± 0.00	0.0 ± 0.00	9 ± 0.2	3 ± 0.1	2 ± 0.0	1073 ± 25.1	498 ± 18.7	371 ± 15.5

* P = petrol, D = Diesel, C = Compact SUV, L = Large SUV

To assess the relative emissions performance of Australian SUVs, the results from this study were compared with other light-duty vehicle PEMS studies (Table 6). These real-world studies reflect a diversity of driving conditions, topographical characteristics (road gradient), meteorological conditions, vehicle emission standards and fuel quality requirements, inspection and maintenance practice. Therefore, the uncertainty in the emission factors is explicitly considered in this comparison and PEMS data were collated from publications in which emission factors and associated uncertainty information were presented.

Table 6 – Overview of PEMS studies with emission factor data with associated uncertainty for comparison with this study.

PEMS Study	Country Region	Vehicle Class	Euro Standards	Pollutants	Uncertainty
De Vlieger, 1997	EU	PC-P	1	NO_x, THC	BV
Daham *et al*., 2009	UK	PC-P	Pre-, 1-4	CO_2, NO_x, THC	WV
Weiss *et al*.,2011	EU	LCV-D/LCV-P	3-5	CO_2, NO_x	BV
Weiss *et al*.,2012	EU	PC-D	4-5	CO_2, NO_x	BV
Hadavi *et al.*, 2012	UK	LCV-D	3	CO_2, NO_x, THC	WV
O'Driscoll *et al*., 2016	UK	PC-D	6	NO_x, NO_2	BV
Valverde *et al*., 2019	EU	PC-P/PC-D	6	CO_2, NO_x, PN, CO	BV
Triantafyllopoulos et al., 2019	EU	PC-D	6	CO_2, NO_x	BV/WV
Kuschel *et al*., 2019; Smit *et al*., 2021	NZ	SUV-P/SUV-D/LCV-D	1,3,4,5	CO_2, NO_x, PM, CO	BV
This study	AUS	SUV-P/SUV-D	5	CO_2, CO, NO, NO_2, PN, CH_4, NMHC	BV/WV

EU = European Union, UK = United Kingdom, NZ = New Zealand, AUS = Australia; PC-P = petrol passenger car, PC-D = diesel passenger car; SUV-P = petrol SUV, SUV-D = diesel SUV, LCV-P = petrol light commercial vehicle, LCV-D = diesel light commercial vehicle;

Uncertainty: Between Vehicle (BV), Within Vehicle (WV).

The estimation of uncertainty in emission factors needs to consider both 'between vehicle' variability (multiple tests with different vehicles) and 'within vehicle' variability (repeat tests with the same vehicle). Within-vehicle variability is of particular interest for PEMS data because variability in test conditions may be a significant additional source of uncertainty, in comparison with, for instance, laboratory-controlled emission tests. For studies where both within and between variability was quantified, a statistical random effects meta-analysis approach was used (Deeks *et al*., 2019) to compute the 95% confidence intervals of the (weighted) mean emission factors. For studies where only ‘between vehicle’ variability (multiple tests with different vehicles) or ‘within vehicle’ variability (single vehicle representative of a vehicle class) were available, confidence intervals were calculated using the conventional parametric method.

The results for petrol LDVs are shown in Figure 6 for selected pollutants. Charts for all pollutants are provided in the Supplementary Material (SM9).

Figure 6 shows that the three Australian petrol SUVs tested in this study exhibit relatively low NO_x and THC emission factors in all driving conditions, when compared with passenger cars (Euro 4 or earlier) that were tested in other international PEMS studies. The average NO_x performance of the three Australian petrol SUVs (URB = 51 mg/km, RUR = 22 mg/km, MWY = 17 mg/km) is comparable to the average NO_x performance reported by Valverde *et al*. (2019) for five Euro 6b passenger cars (URB = 75 mg/km, RUR = 48 mg/km, MWY = 20 mg/km). The results presented in SM9 show that NO_x emission performance of Australian petrol SUVs is at the low end of reported international values, which are generally significantly higher albeit for older emission standards. The CO_2 emission factor for Australian petrol SUVs (URB = 335 g/km, RUR = 162 g/km, MWY = 128 g/km) is about a factor of two higher in urban conditions, but similar in motorway conditions. The results presented in SM9 show that emissions performance of the three Australian petrol SUVs is generally within the range of values reported in international studies for CO_2.

CO emissions appear relatively high in urban (2.5 g/km) and rural conditions (1.3 g/km) and low in motorway conditions (0.2 g/km), but the results could only be compared with one other study (Valverde *et al.*, 2019), with corresponding values of 0.3 g/km, 0.4 g/km and 1.7 g/km, respectively. THC emissions also seem low for the Australian petrol SUVs across all driving conditions ranging from about 10 to 30 mg/km, but comparison is made with older Euro standards (pre-Euro to Euro 4), ranging from 70 to 2200 mg/km. Finally, PN emissions appear similar albeit lower in urban conditions (10×10^{11} #/km), rural conditions (6×10^{11} #/km) and motorway conditions (2×10^{11} #/km), but the results could only be compared with one other study (Valverde *et al.*, 2019), with corresponding values of 13×10^{11} #/km, 7×10^{11} #/km and 12×10^{11} #/km, respectively.

In conclusion, the three Australian petrol SUVs appear to perform well for air pollutant emissions from an international perspective and are within the observed range of on-road greenhouse gas (CO_2) emission rates.

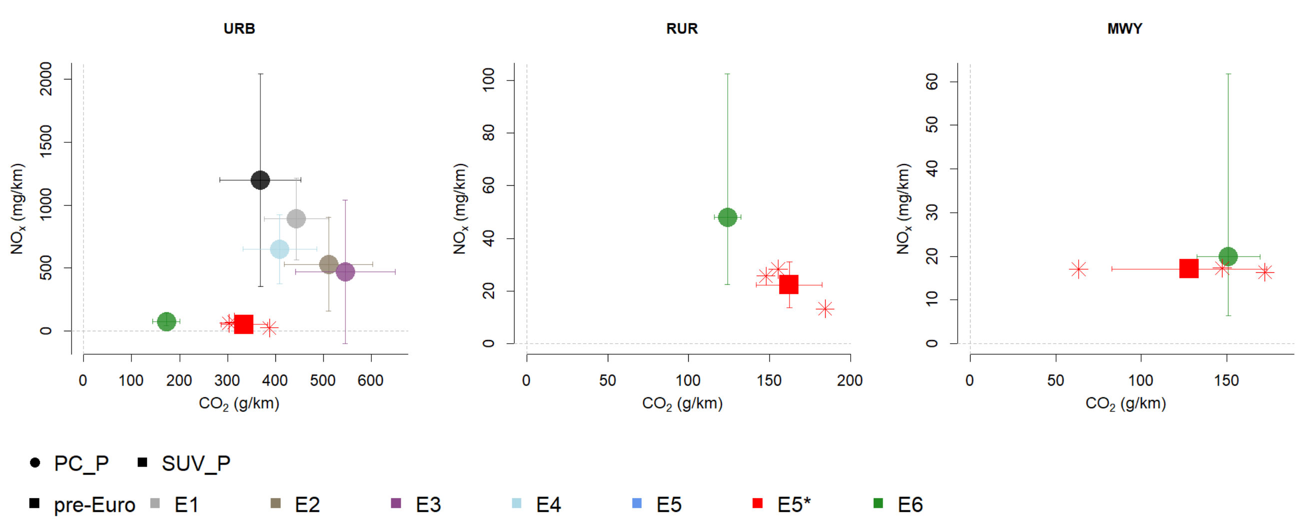

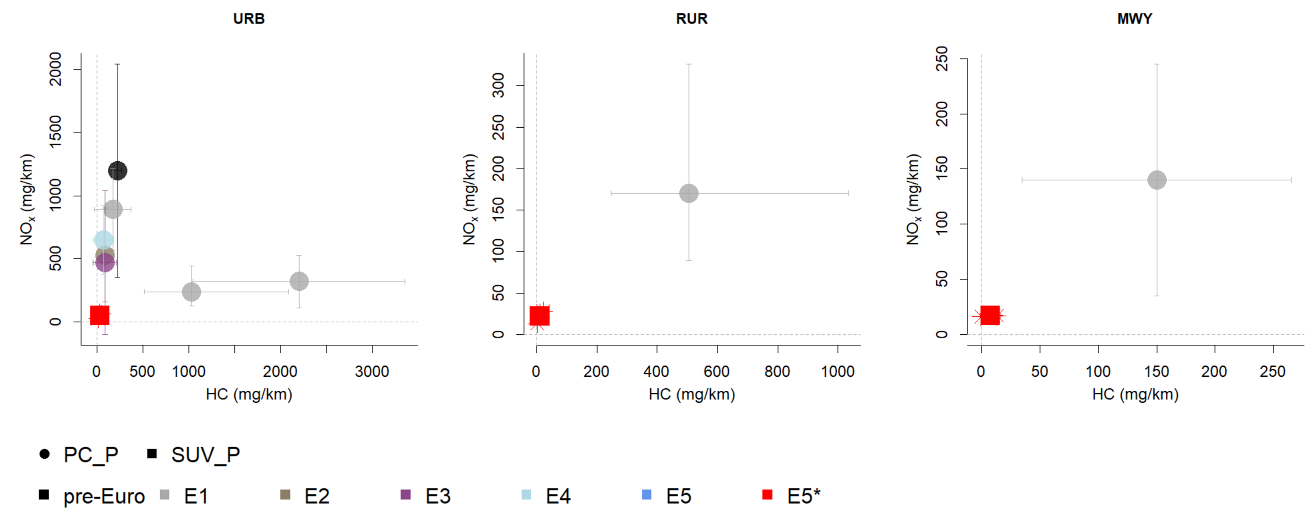

Figure 6 – Petrol LDVs – comparison of CO_2 THC and NO_x mean emission factors and 95% confidence interval derived from PEMS measurements in this study and from international studies listed in Table 6. The results from this study are shown with a red square. Individual mean SUV test (n = 3) results from this study are also shown with an * symbol in the charts.

The results for diesel LDVs are shown in Figure 7 for selected pollutants. Charts for all pollutants are provided in the Supplementary Material (SM9). Regarding CO_2 emissions performance, Australian diesel SUVs have considerably higher emissions as compared with Euro 3 LCVs (Hadavi *et al*., 2012) and Euro 6 PCs tested in Europe (Triantafyllopoulos *et al*., 2019; Valverde *et al*., 2019), but overall similar performance when compared with New Zealand SUVs and LCVs (Kuschel *et al*., 2019). The European LDV data suggest average on-road CO_2 emission factors of about 170 g/km (Urban), 122 g/km (Rural) and 160 g/km (Motorway). The Australian SUVs have average CO_2 emission factors of 355 g/km

(Urban), 185 g/km (Rural) and 194 g/km (Motorway), so 20% to 110% higher than the EU LDVs depending on traffic conditions.

The two diesel SUVs tested in this study exhibit high NO_x emission rates in real-world urban and rural driving conditions. For instance, in urban conditions, the average NO_x emission factor is 2.2 g/km for the Australian Euro 5 diesel SUVs, which is higher than 1.8 g/km reported for older technology Euro 3 LCVs (Hadavi *et al*., 2012) and substantially higher compared with Euro 6 technology vehicles, where a range of 0.4 to 0.8 g/km has been reported (O'Driscoll *et al*., 2016; Triantafyllopoulos *et al*., 2019; Valverde *et al*., 2019). The Australian results for NO_x are comparable to PEMS testing done in New Zealand (Kuschel *et al*., 2019; Smit *et al*., 2021), where the results for range from 1.6 g/km (Euro 4 LCV) to 2.6 g/km (Euro 4 SUV). The Australian SUVs have the highest NO_x emission factor in rural conditions (0.9 g/km) as compared with Euro 4 (0.7 – 0.8 g/km, Kuschel *et al*., 2019; Smit *et al*., 2021) and Euro 6 (0.6 g/km, Triantafyllopoulos *et al*., 2019; Valverde *et al*., 2019) technology. For motorway conditions, the NO_x emission factor for Australian SUVs (0.7 g/km) is within the range of reported values for Euro 6 technology cars, 0.3 – 1.0 g/km (O'Driscoll *et al*., 2016; Triantafyllopoulos *et al*., 2019; Valverde *et al*., 2019). The data suggest that there is no improvement in NO_x emissions performance of Australian Euro 5 diesel SUVs in urban and rural conditions, as compared with older Euro technology in other countries.

Figure 6 shows that the average NO_2 emission factors for the Australian SUVs (334, 170, 148 mg/km) in urban, rural and motorway conditions, are generally within the range of or close to European (150 – 367 mg/km) and New Zealand (221 – 717 mg/km) on-road tests (Hadavi *et al*., 2012; O'Driscoll *et al*., 2016; Kuschel *et al*., 2019; Smit *et al*., 2021). As a consequence, NO_2/NO_x ratios are relatively low for the Australian diesel SUVs (15–20%), which is comparable with older Euro technology: 20% for Euro 3

(Hadavi *et al.*, 2012) and 24 –30% for Euro 4 (Kuschel *et al.*, 2019; Smit *et al.*, 2021), but significantly different from Euro 6 technology with about 50% (O'Driscoll *et al.*, 2016).

There is limited international data available for comparison of CO, THC and PN emission rates. The charts presented in SM9 show that emissions performance of the two diesel SUVs is very low for CO and THC. For PN emissions, the results could only be compared with one other study that tested Euro 6 vehicles (Valverde *et al.*, 2019) and reported 0.16×10^{11} #/km (urban), 0.01×10^{11} #/km (rural) and 0.02×10^{11} #/km (motorway). PN emission factors determined in this study are similar in motorway conditions (0.01×10^{11} #/km) but are substantially higher in rural conditions (0.66×10^{11} #/km) and motorway conditions (5.23×10^{11} #/km).

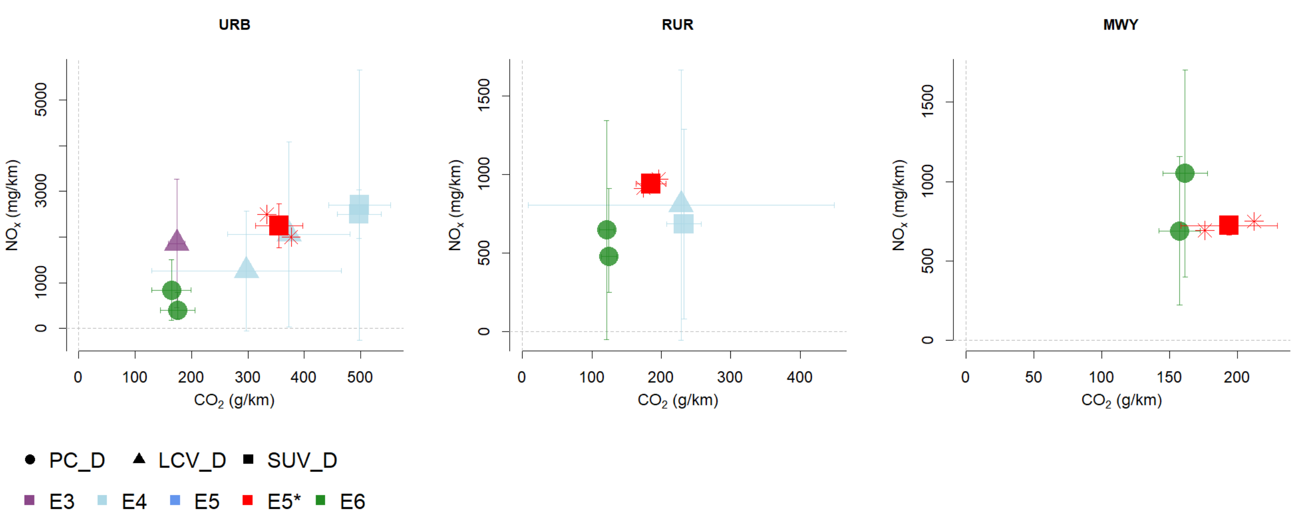

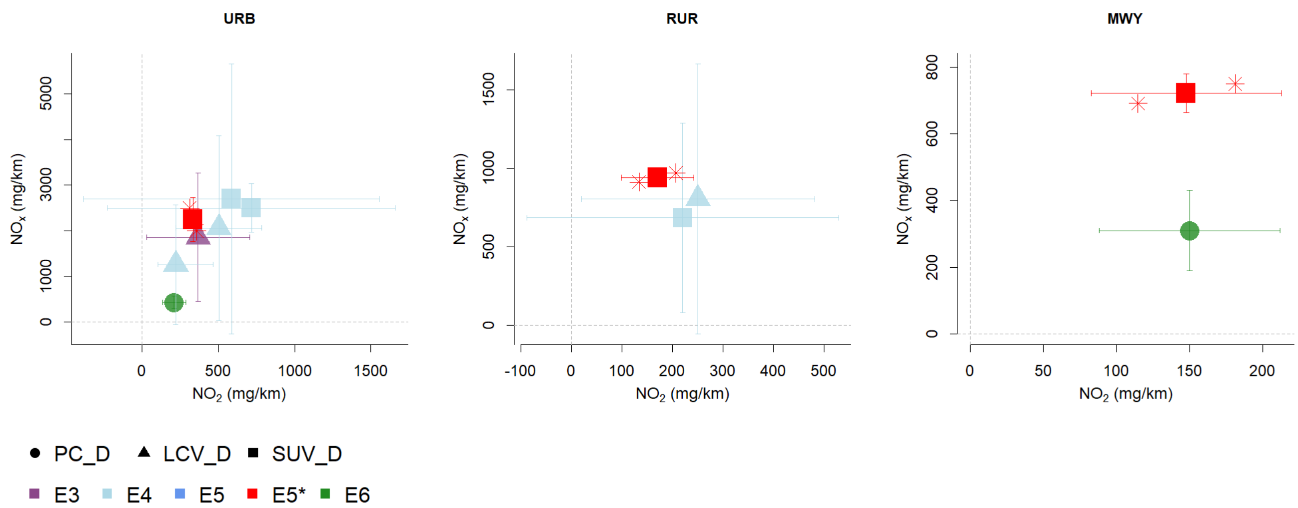

Figure 7 – Diesel LDVs – comparison of CO_2, NO_x and NO_2 mean emission factors and 95% confidence interval derived from PEMS measurements in this study and from international studies listed in Table 6. The results from this study are shown with a red square. Individual mean SUV test (n = 3) results from this study are also shown with an * symbol in the charts.

4.3 – Manoeuvre-based emission factors (hot running average speed)

Figures 8 and 9 compare the average speed hot running emission factor algorithms created in this study from processed PEMS data with current COPERT Australia v1.3.5 emission factors for three SUV vehicle classes. Performance statistics were computed including the coefficient of determination (R^2), the normalised root mean square error (NRMSE) and the mean prediction error (MPE). The results are shown in Table 7.

Figure 8 shows that the fitted emission factor algorithms for CO_2 compare well with current COPERT Australia emission factors, suggesting no further correction is required. Table 7 confirms consistency with NRMSE varying from 10-15%, R^2 around 90% and MPE between 7 and 40 g/km (COPERT overpredicts).

COPERT Australia performs reasonably well for NO_x for petrol SUVs with a MPE of about ± 10 mg/km, an NRMSE varying from about 20-30% and R^2 around 99%, although the shape of the speed-emission factor relationship for large petrol SUVs is significantly flatter. The measurements suggest that NO_x for compact petrol SUVs is underestimated by 8 mg/km by COPERT Australia and overestimated by 11 mg/km for large petrol SUVs.

In contrast, PEMS measurements suggest that COPERT Australia emission factors for diesel SUVs are underestimated with a large margin of about 1.2 g/km, on average a factor of seven higher (NRMSE). The same applies to NO_2, where the PEMS data suggest COPERT Australia emission factors for diesel SUVs are biased and underestimate emission factors by 178 mg/km, on average a factor of three higher (NRMSE). Significant bias and underestimation of COPERT Australia NO_2 emission factors are also visible in Figure 6 for petrol SUVs (NRMSE: factor of three to five), albeit significantly smaller with an MPE of 3 to 4 mg/km.

The PEMS measurements suggest large deviations from the COPERT Australia emission factors for CO and THC in terms of shape of the relationship with average speed, as well as absolute and relative values (NRMSE 27% to 352%). Measured CO emissions in particular are significantly higher than the COPERT Australia emission factors for petrol SUVs. The THC results for diesel are more reasonable with a NRMSE of 27% and an average overestimation of 5 mg/km. There is a general tendency for elevated emissions of these pollutants in urban conditions, which is not shown in the COPERT Australia average speed – emission factor relationships.

Logistic functions (for instance, reverse sigmoid) are not used in COPERT, but this study suggest they can lead to improved prediction algorithms, as is evident in Figure 8 (NO_x SUV Diesel, NO_2 SUV-L Petrol) and Figure 9 (THC and CH_4 SUV-C Petrol). Expanding the flexibility of different mathematical algorithms is recommended for future COPERT updates.

Table 7 – COPERT Australia prediction performance

Class	Pollutant	R^2 (-)	NRMSE (%)	MPE	(Units MPE)
SUV-C-petrol	CO_2	0.90	12%	-25	g/km
SUV-L-petrol		0.87	11%	-7	
SUV-diesel		0.91	14%	-40	
SUV-C-petrol	NOx	0.99	19%	8	mg/km
SUV-L-petrol		0.99	32%	-11	
SUV-diesel		0.24	624%	1215	
SUV-C-petrol	NO_2	0.99	429%	4	mg/km
SUV-L-petrol		0.89	278%	3	
SUV-diesel		0.35	305%	178	
SUV-C-petrol	CO	0.77	352%	1591	mg/km
SUV-L-petrol		0.75	180%	598	
SUV-diesel		0.97	55%	-111	
SUV-C-petrol	THC	0.74	273%	13	mg/km
SUV-L-petrol		0.91	149%	-8	
SUV-diesel		0.74	27%	-5	

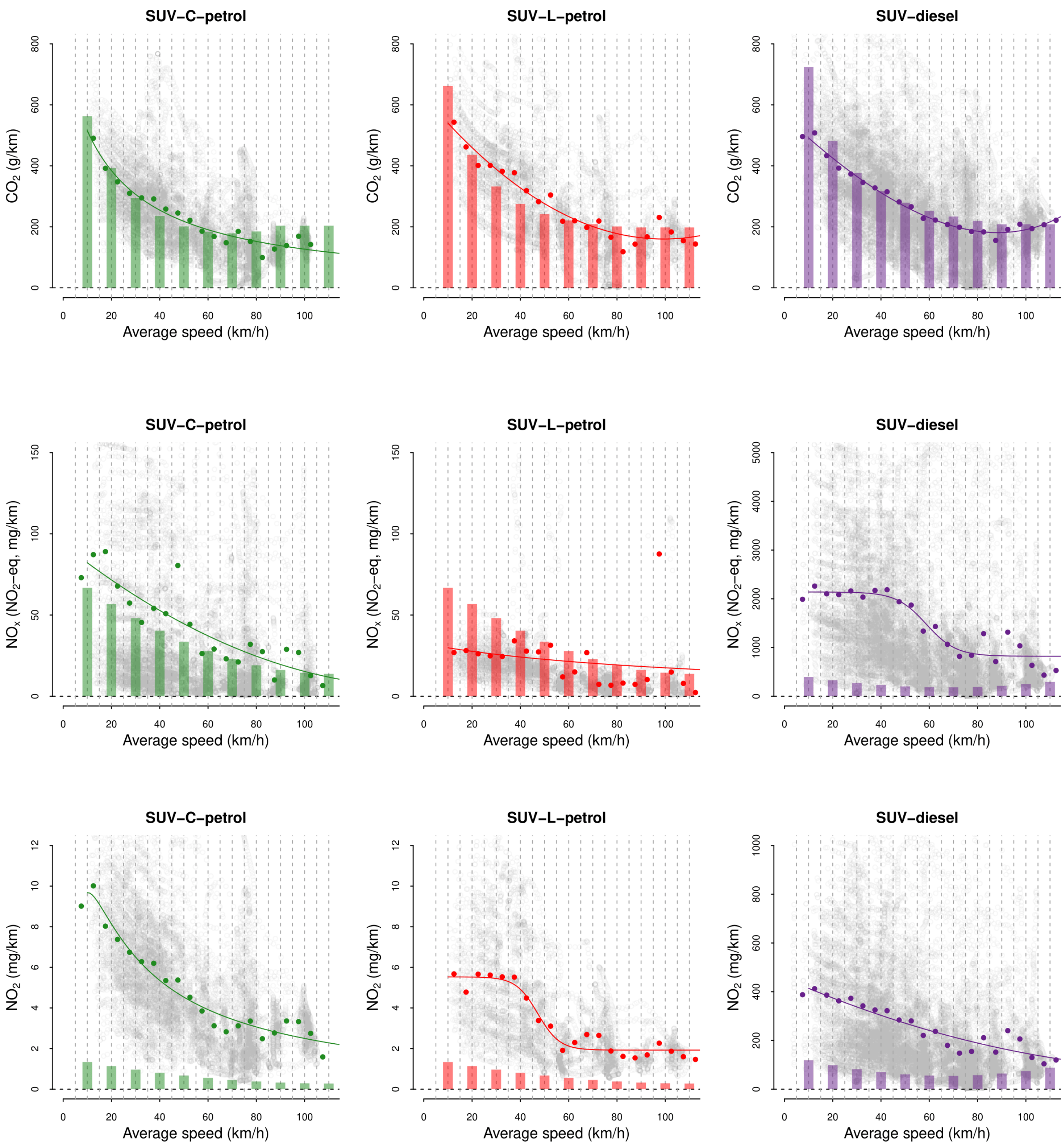

Figure 8 – Comparison of CO_2, NO_x and NO_2 mean emission factor predictions by this study (regression line) and COPERT Australia v1.3.5. (bars) for three SUV vehicle classes. Manoeuvre-based emission factors are shown as light grey open dots. Bin averaged emission factor values are shown as solid dots.

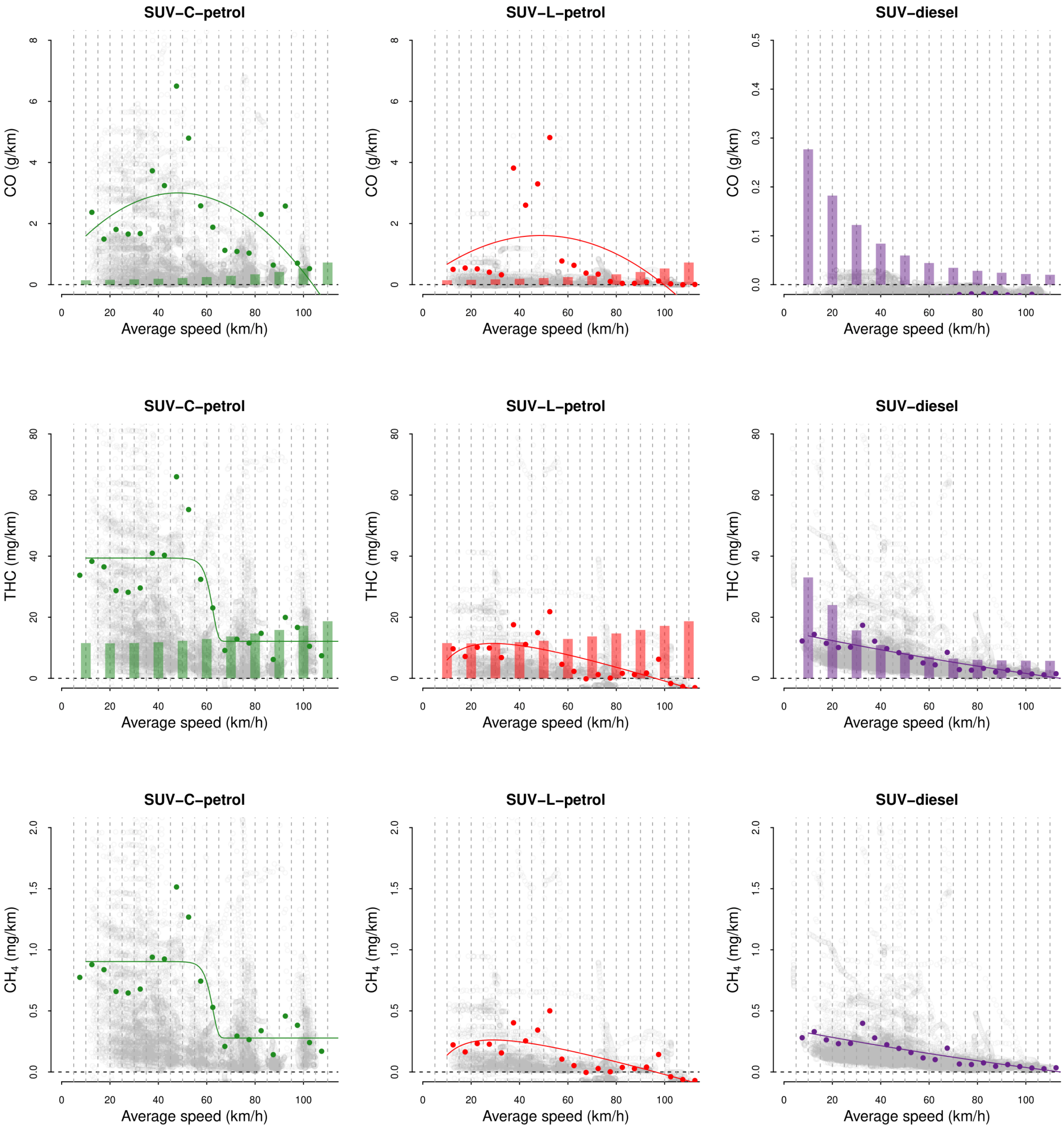

Figure 9 – Comparison of CO, THC and CH_4 mean emission factor predictions by this study (regression line) and COPERT Australia v1.3.5. (bars, if available) for three SUV vehicle classes. Manoeuvre-based

emission factors are shown as light grey open dots. Bin averaged emission factor values are shown as solid dots.

4.4 – Extended idling

Idling may be expected to result in approximately constant fuel consumption and emission rates, independent of the idling period. Time-series charts are presented in the Supplementary Material (SM10) for all pollutants and vehicles. They include second-by-second emission traces and exhaust temperature profiles. It is noted that exhaust temperature gradually drops about 20 to 60 °C, depending on the vehicle, as shown in SM10. The time-series charts presented in SM10 show that is generally the case for CO_2 for all test vehicles. However, for the air pollutant emissions, the results vary significantly. For some specific combinations of test vehicle and pollutant, emission profiles exhibit significant non-linear changes over time, sometimes without an obvious trend (Figure 10). It is likely that these changes are the result of complex interactions between, for instance, a steady reduction in catalyst temperature and changes in engine management (e.g. changes in fuel injection strategy).

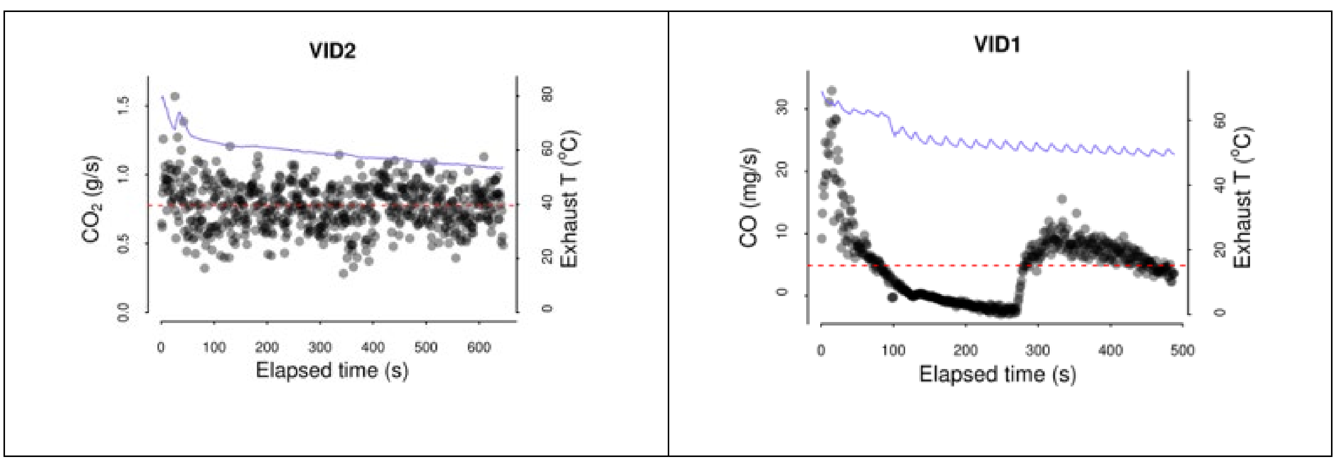

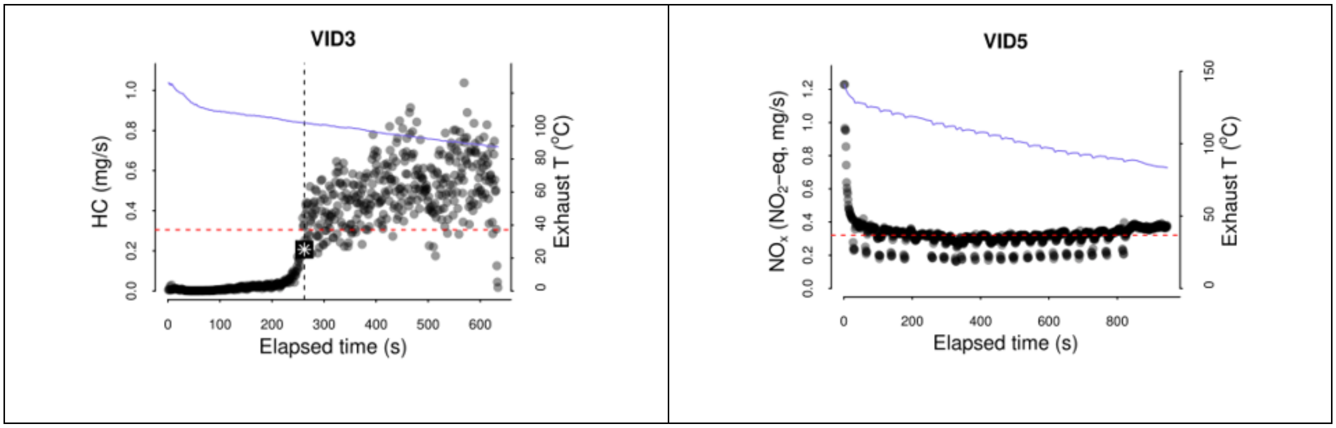

Figure 10 – Some examples of steady and erratic idling emissions behaviour (black dots) over time. Exhaust temperature is shown as a purple solid line and the grand mean emission rate as a horizontal dashed red line.

Table 8 shows the idling results for the individual vehicles. An assessment of structural change is included. A *p*-value < 0.05 provides evidence for the alternative hypothesis (structural change) over the null hypothesis (no structural change), and this is indicated with a * symbol in Table 8. The statistical test results indicate that non-constant emissions behaviour over time can be detected in almost all situations, except for PN emissions for VID 4 and VID 5. Idling emission rates can show significant changes over time during prolonged idling events.

Table 8 shows that the SUVs emit, on average, 0.5 to 0.9 g CO_2 per second, while idling after driving in urban conditions for about 10 minutes, which translates to 0.3 to 0.5 kg of accumulated CO_2 emissions after 10 minutes of idling. Avoidance of idling will generate immediate GHG emission benefits.

For air pollutant emissions, the point in time where cumulative idling emissions are equivalent to hot start emissions could be determined for only eight vehicle-pollutant combinations, and mainly for THC.

Continued idling after this point in time will increase net emissions when additional restart emissions are considered. Prevention of idling periods shorter than this time will generate an emissions benefit.

Table 8 shows that the variability in time points is large, spanning from 19 seconds to 9.6 hours. They depend on the pollutant and test vehicle. For THC emissions, the data presented in Table 8 suggest idling less than 19 seconds to 6 minutes will generate a net emission benefit when start emissions are accounted for. This vehicle-to-vehicle and pollutant dependent variability complicates generic statements on the benefits of idle reduction for air pollutants. On the other hand, the benefits of idle reduction for greenhouse gas emission reduction are clear as vehicles stop emitting once the engine is turned off.

Table 8 – SUV idling emission factors by vehicle and pollutant, including assessment of structural change in the time-series data where * indicates a significant structural change ($p < 0.05$) and hot start equivalence point in time.

	CO_2 (g/s)			NO_x (mg/s)			NO_2 (mg/s)		
VEHICLE ID *	Emission Factor	Structural Change	Hot Start Equivalence	Emission Factor	Structural Change	Hot Start Equivalence	Emission Factor	Structural Change	Hot Start Equivalence
VID 1 (C, P)	0.902	*	-	0.452	*	5 min	0.023	*	-
VID 2 (C, P)	0.777	*	-	0.018	*	45 min	0.019	*	-
VID 3 (L, P)	0.565	*	-	0.004	*	-	0.007	*	-
VID 4 (C, D)	0.492	*	-	2.635	*	-	0.548	*	-
VID 5 (L, D)	0.575	*	-	0.271	*	-	0.085	*	-

	CO (mg/s)			THC (mg/s)			PN (10^{11} #/s)		
VEHICLE ID *	Emission Factor	Structural Change	Hot Start Equivalence	Emission Factor	Structural Change	Hot Start Equivalence	Emission Factor	Structural Change	Hot Start Equivalence
VID 1 (C, P)	4.886	*	22 min	0.094	*	6 min	0.006	*	-
VID 2 (C, P)	0.406	*	-	0.017	*	-	0.000	*	9.6 hours
VID 3 (L, P)	0.070	*	-	0.305	*	4 min	0.000	*	-

VID 4 (C, D)	-0.166	*	-	0.038	*	19 sec	0.000		-
VID 5 (L, D)	-0.033	*	-	0.015	*	33 sec	0.000		-
		CH_4 (mg/s)			NMHC (mg/s)			NO (mg/s)	
VEHICLE ID *	Emission Factor	Structural Change	Hot Start Equivalence	Emission Factor	Structural Change	Hot Start Equivalence	Emission Factor	Structural Change	Hot Start Equivalence
VID 1 (C, P)	0.002	*	-	0.092	*	-	0.280	*	-
VID 2 (C, P)	0.000	*	-	0.016	*	-	-0.001	*	-
VID 3 (L, P)	0.007	*	-	0.299	*	-	-0.002	*	-
VID 4 (C, D)	0.001	*	-	0.037	*	-	1.361	*	-
VID 5 (L, D)	0.000	*	-	0.015	*	-	0.121	*	-

* P = petrol, D = Diesel, C = Compact SUV, L = Large SUV

5. Conclusions

This study has undertaken PEMS measurements from five SUVs to address the lack of quality-controlled emissions data in the Australian context. Vehicles were tested under cold start, hot start and extended idling conditions. Fuel quality and coastdown testing were incorporated into our study design as well. Diesel SUVs reproduced the Euro 5 NOx problem, with emission factors (on average) being seven times the relevant type approval limit. We recommend that the COPERT Australia emission algorithms be updated to reflect the findings of this study, although we note that CO_2 emission factors are accurate and do not require modification. We suggest that further PEMS studies be carried out to more comprehensively assess emissions from international vehicle fleets that rely on a range of automotive technologies.

Acknowledgements

The authors thank Ms Nicole Debenham from TAFE NSW for access to the parade ground at the Nirimba Education Precinct for vehicle coastdown testing. This work was funded by the Queensland Department of Environment and Science.

6. References

- ABMARC. 2017. The Real World Driving Emissions Test – 2017 Fuel Economy and Emissions Report, Melbourne, Australia, pp 1-20.
- Andrews, D.W., Ploberger, W., 1994. Optimal tests when a nuisance parameter is present only under the alternative, *Econometrica: Journal of the Econometric Society*, 1383-1414.

- Boriboonsomsin, K., Barth, M., 2009. Impacts of road grade on fuel consumption and carbon dioxide emissions evidenced by use of advanced navigation systems, Transportation Research Record 2139, Transportation Research Board of the National Academies, Washington D.C., USA, 21–30.
- Calcagno, J.A., 2005. *Evaluation of Heavy-Duty Diesel Vehicle Emissions During Cold-Start and Steady-State Idling Conditions and Reduction of Emissions from a Truck-Stop Electrification Program*, PhD dissertation, University of Tennessee, 2005, https://trace.tennessee.edu/utk_graddiss/1892.
- Daham, B., Li, H., Andrews, G.E., Ropkins, K., Tate, J., Bell, M.C., 2009. Comparison of real-world emissions in urban driving for Euro 1-4 vehicles using a PEMS, *SAE Technical Paper Series*, 2009-01-0941.
- De Vlieger, 1997. On-board emission and fuel consumption measurement campaign on petrol-driven passenger cars, *Atmospheric Environment*, 31 (22), 3753- 3761.
- Deeks, J.J., Higgins, J.P.T., Altman, D.G. (Eds.), 2019. *Chapter 10: Analysing Data and Undertaking Meta-analyses, Cochrane Handbook for Systematic Reviews of Interventions version 6.0 (updated July 2019)*, www.training.cochrane.org/handbook.
- Dong, C., Zeng, H., Chen, M., 2014. A cost efficient online algorithm for automotive idling reduction, *Proceedings 2014 Design Automation Conference*, No. 2593070.
- EC, 2017. Commission Regulation (EU) 2017/1151, 1 June 2017, European Commission.

- EC, 2018. Commission Regulation (EU) 2018/1832, 5 November 2018, European Commission.
- Favez, J., Weilenmann, M., Stilli, J., 2009, Cold start extra emissions as a function of engine stop time: evolution over the last 10 years, Atmospheric Environment, 43, 996-1007.
- Fontaras, G., Zacharof, N.G., Ciuffo, B., 2017. Fuel consumption and CO2 emissions from passenger cars in Europe – Laboratory versus real-world emissions. Progress in Energy and Combustion Science, 60, 97–131. https://doi.org/10.1016/j.pecs.2016.12.004.
- Frey, H.C., Zhang, K., Rouphail, N.M., 2008. Fuel use and emissions comparisons for alternative routes, time of day, road grade, and vehicles based on in-use measurements, Environ. Sci. Technol., 42, 2483–2489.
- Gallus, J., Kirchner, U., Vogt, R., Benter, T., 2017. Impact of driving style and road grade on gaseous exhaust emissions of passenger vehicles measured by a Portable Emission Measurement System (PEMS), Transportation Research Part D, 52, 215–226.
- Geoscience Australia, 2021. Elevation Information System, Online Data, http://www.ga.gov.au/scientific-topics/national-location-information/digital-elevation-data.
- Giechaskiel, B. et al. 2016. Implementation of portable emissions measurement systems (PEMS) for the real-driving emissions (RDE) regulation in Europe. Journal of Visualized Experiments, 118, Article Number e54753. doi: 10.3791/54753.

- Hadavi, S., Li, H., Przybyla, G., Jarrett, R., Jarrett, R., Andrews, G., 2012. Comparison of gaseous emissions for B100 and diesel fuels for real-world urban and extra urban driving, *SAE Int. J. Fuels Lubr.*, 5(3), doi:10.4271/2012-01-1674, 1132-1154.
- James, G., Witten, D., Hastie, T., Tibshirani, R., 2017. *An Introduction to Statistical Learning – With Applications in R*, Springer New York, USA, ISBN 978-1-4614-7138-7, DOI 10.1007/978-1-4614-7138-7.
- Katsis, P., Smit, R., Ntziachristos, L., Lo, T.S., Wong, C., 2016. Quality assurance of PEMS emissions data aimed for the development of real-world emission factors, 21st Transport and Air Pollution Conference, 24-26 May 2016, Lyon, France.
- Kent, J. H., Allen, G. H., Rule, G. 1978. A driving cycle for Sydney. *Transportation Research*, 1978, 12(3), pp. 147–152.
- Kent, J. H.,Mudford, N. R. 1979. Motor vehicle emissions and fuel consumption modelling. *Transportation Research Part A: General*, 1979, 13(6), pp. 395–406.
- Killick, R., Eckley, I.A., 2013. changepoint: An R Package for Changepoint Analysis, *Journal of Statistical Software*, June 2014, 58 (3), 1-19.
- Kuschel, G., Metcalfe, J., Baynham, P., Wells, B., 2019. *Testing New Zealand Vehicles to Measure Real-World Fuel Use and Exhaust Emissions*, NZ Transport Agency Research Report 658, 121 pp.
- Lovelace, R., Nowosad, J., Muenchow, J., 2019. Geocomputation with R, CRC Press, ISBN 978-1-138-30451-2.

- Lust, E.E., Horton, W.T., Radermacher, R., 2008. A review and cost comparison of current idle-reduction technology, *Proceedings of POWER2008*, ASME Power 2008, 22-24 July 2008, Orlando, Florida, USA.
- O'Driscoll, R., ApSimon, H.M., Oxley, T., Molden, N., Stettler, M.E.J., Thiyagarajah, A., 2016. A Portable Emissions Measurement System (PEMS) study of NO_x and primary NO_2 emissions from Euro 6 diesel passenger cars and comparison with COPERT emission factors, *Atmospheric Environment*, 145, 81-91.
- R Core Team, 2017. R: A language and environment for statistical computing. R Foundation for Statistical Computing, Vienna, Austria. URL https://www.R-project.org/
- R Studio Team, 2015. RStudio: Integrated Development Environment for R, Boston, MA. Available at: http://www.rstudio.com/
- Samaras, Z., Geivanidis, S., 2005. *Speed Dependent Emission and Fuel Consumption Factors for Euro Level Petrol and Diesel Passenger Cars*, Report 0417, Laboratory of Applied Thermodynamics, Aristotle University Thessaloniki, Greece, May 2005, DG TREN 1999-RD.10429.
- Shancita, I., Masjuki, H.H., Kalam, M.A., Rizwanul Fattah, I.M., Rashed, M.M., Rashedul, H.K., 2014. A review on idling reduction strategies to improve fuel economy and reduce exhaust emissions of transport vehicles, *Energy Conversion and Management*, 88, 794–807.

- Smit, R., Ntziachristos, L., 2012. COPERT Australia: developing improved average speed vehicle emission algorithms for the Australian Fleet, *19th International Transport and Air Pollution Conference*, Thessaloniki, Greece, 26-27 November 2012.
- Smit, R., 2013a. Development and performance of a new vehicle emissions and fuel consumption software (PΔP) with a high resolution in time and space, Atmospheric Pollution Research, 4, 336-345.
- Smit, R., 2013b. A procedure to verify large modal vehicle emissions databases, CASANZ 2013 Conference, Sydney, 7-11 September 2013.
- Smit, R., Ntziachristos, L., 2013. Cold start emission modelling for the Australian petrol fleet, Air Quality and Climate Change, 47 (3), 31-39.
- Smit, R., Kingston, P., 2019. Detecting cold start vehicles in the on-road fleet, Air Quality and Climate Change, 53 (1), March 2019, 22-26.
- Smit, R., Bluett, J., Pearce, S., Van Vugt, A., Bagheri, S., 2021. Determining the Impact of Vehicle Emissions on Harmful and GHG Through In-Use Vehicle Emission Monitoring – Stage1, Waka Kotahi NZ Transport Agency Research Report [###], 121 pp.
- Society of Automotive Engineers. 2010. Road Load Measurement and Dynamometer Simulation using Coastdown Techniques, SAE J1263, SAE International, USA.

- TER, 2019. *Real-World CO_2 Emissions Performance of the Australian New Passenger Vehicle Fleet 2008-2018 – Impacts of Trends in Vehicle/Engine Design*, Transport Energy/Emission Research (TER), 14 September 2019. https://www.transport-e-research.com/publications.
- TER, 2020. *Motor Vehicle Engine Idling in Australia – a critical review and initial assessment,* Transport Energy/Emission Research (TER), 12 June 2020. https://www.transport-e-research.com/publications.
- TNO, 2005. The Effects of Idling Engines on Emissions and Local Air Quality, (In Dutch: De Effecten van Stationair Draaiende Motoren Emissies van Wegverkeer en Lokale Luchtkwaliteit), by Smit, R., Vermeulen, R., Wesseling, J., Smokers, R., TNO Report 05.OR.VM.036.1/RS, 11 November 2005.
- Triantafyllopoulos, G., Dimaratos, A., Ntziachristos, L., Bernard, Y., Dornoff, J., Samaras, Z., 2019. A study on the CO2 and NOx emissions performance of Euro 6 diesel vehicles under various chassis dynamometer and on-road conditions including latest regulatory provisions, Science of the Total Environment, 666, 337–346.
- Valverde, V., Mora, B.A., Clairotte, M., Pavlovic, J., Suarez-Bertoa, R., Giechaskiel, B., Astorga-Llorens, C., Fontaras, G., 2019. Emission factors derived from 13 Euro 6b light-duty vehicles based on laboratory and on-road measurements, *Atmosphere*, 10, 243, doi:10.3390/atmos10050243.
- Velleman, P.F., 1980. Definition and Comparison of Robust Nonlinear Data Smoothing Algorithms, Journal of the American Statistical Association, 75, 371, 609-615.

- Weiss, M., Bonnel, P., Hummel, R., Provenza, A., Manfredi, U., 2011. On-Road Emissions of Light-Duty Vehicles in Europe, *Environ. Sci. Technol.*, 45, 8575–8581.
- Weiss, M., Bonnel, P., Kühlwein, J., Provenza, A., Lambrecht, U., Alessandrini, S., Carriero, M., Colombo, R., Forni, F., Lanappe, G., Le Lijour, P., Manfredi, U., Montigny, F., Sculati, M., 2012. Will Euro 6 reduce the NO_x emissions of new diesel cars? - Insights from on-road tests with Portable Emissions Measurement Systems (PEMS), *Atmospheric Environment*, 62, 657-665.
- **White, R. A. and Korst, H. H. 1972. The determination of vehicle drag contributions from coast-down test. SAE Technical Paper 720099.**
- Wong, C.K.L., Lo, T.S., Wong, H.L.A, Lam, K.L., Frey, H.C., Smit, R., Hausberger, S., Weller, K., Ntziachristos, L., 2019., Microscale vehicle emission modelling in Hong Kong, 23rd Transport and Air Pollution Conference, 15-17 May 2019, Thessaloniki, Greece.
- Zeileis, A., Leisch, F., Hornik, K., Kleiber, C., 2002. strucchange: An R Package for Testing for Structural Change in Linear Regression Models, *Journal of Statistical Software*, January 2002, 7 (2), 1-38.